NATIONAL ADVISORY COMMITTEE FOR AERONAUTICS

WARTIME REPORT

ORIGINALLY ISSUED
April 1945 as
Advance Restricted Report L5C13a

INVESTIGATION OF EFFECT OF SIDESLIP ON LATERAL STABILITY CHARACTERISTICS III - RECTANGULAR LOW WING ON CIRCULAR FUSELAGE WITH VARIATIONS IN VERTICAL-TAIL AREA AND FUSELAGE LENGTH WITH AND WITHOUT HORIZONTAL TAIL SURFACE

By Thomas A. Hollingworth

Langley Memorial Aeronautical Laboratory
Langley Field, Va.

NACA

WASHINGTON

NACA ARR No. L5C13a [redacted]

NATIONAL ADVISORY COMMITTEE FOR AERONAUTICS

ADVANCE RESTRICTED REPORT

INVESTIGATION OF EFFECT OF SIDESLIP ON LATERAL STABILITY CHARACTERISTICS III - RECTANGULAR LOW WING ON CIRCULAR FUSELAGE WITH VARIATIONS IN VERTICAL-TAIL AREA AND FUSELAGE LENGTH WITH AND WITHOUT HORIZONTAL TAIL SURFACE

By Thomas A. Hollingworth

SUMMARY

Power-off tests were made in the 6- by 6-foot test section of the Langley stability tunnel to determine the variation of the static lateral stability characteristics with vertical-tail area, fuselage length, and wing dihedral. Two NACA 23012 rectangular wings with rounded tips and dihedral angles of 0° and 5° were tested alone and in combination with three circular fuselages of different lengths. The wing-fuselage combinations were tested as low-wing monoplanes with and without a horizontal tail and with variations in vertical-tail area. The results are presented as curves showing the variation of the static-lateral-stability slopes with angle of attack, and the rolling-moment, yawing-moment, and lateral-force coefficients with angle of yaw.

The results indicated that the influence of wing-fuselage interference on the slope of the curve of yawing-moment coefficient against angle of yaw C_{n_ψ} and the slope of the curve of lateral-force coefficient against angle of yaw C_{Y_ψ} was usually stabilizing, appreciable, and varied with angle of attack. The influence of the wing-fuselage interference on the vertical tail was also generally stabilizing and appreciable at negative and small positive angles of attack but varied with angle of attack.

[redacted]

With no vertical tail, increased fuselage length ordinarily caused a slight increase in C_{n_ψ} for the fuselage lengths tested. At the larger negative angles of attack, this effect was more pronounced. For the complete model, the increase in C_{n_ψ} was approximately linear with fuselage length. The magnitude of this increase appreciably diminished with a positive increase in angle of attack. The slopes C_{n_ψ} and C_{Y_ψ} increased approximately linearly with vertical-tail area. For the system of axes used, the slope of the curve of rolling-moment coefficient against angle of yaw C_{l_ψ} increased with vertical-tail area at negative and small positive angles of attack but the opposite was true at large positive angles of attack. The results also indicated that increased dihedral angle slightly decreased the rate of change of C_{n_ψ} with vertical-tail area but had a negligible effect on the rate of change of C_{n_ψ} with fuselage length. Except at large positive angles of attack, C_{Y_ψ} was generally greater with the smaller dihedral angle. A slight increase in C_{n_ψ} was caused by the end-plate effect of the horizontal tail on the vertical tail.

INTRODUCTION

The trend toward greater speed and higher wing loadings and increased consciousness of the importance of satisfactory flying qualities have resulted in additional attention being given to handling characteristics in airplane design. Mathematical equations and convenient charts for predicting the lateral stability characteristics are given in reference 1. In order to use this material, however, it is necessary to know the stability derivatives, which vary with each airplane configuration. A series of investigations has therefore been undertaken in the Langley stability tunnel to determine the variation of both the static-stability and rotary-stability slopes with various airplane parameters.

The present investigation is a continuation of the investigations described in references 2 and 3 except that, for the present tests, the fuselage was equipped

with a rectangular wing in the low position. The purpose of the investigation, which was conducted in the 6- by 6-foot test section of the Langley stability tunnel, was to determine experimentally the effect, with the propeller off, of vertical-tail area, fuselage length, wing dihedral, interference, and the presence of the horizontal tail on the static lateral stability characteristics. A geometrically similar model has been tested in the Langley 7- by 10-foot tunnel (reference 4) and the data may be used to correlate the results in the two tunnels.

Tests were made of a model that had dimensions proportional to those of the average airplane. The ratios of fuselage length to wing span and of vertical-tail area to wing area investigated were taken to bracket the range commonly used on present-day airplanes.

APPARATUS AND MODEL

The tests were made in the 6- by 6-foot closed-throat test section (adjusted for straight flow) of the Langley stability tunnel. A three-view drawing of the model tested, which was constructed of laminated mahogany, is given in figure 1. Figure 2 shows the model mounted on the three support struts for tests in the tunnel.

The two rectangular wings used for the tests have dihedral angles of 0° and 5° and, in elevation, the maximum upper-surface section ordinates are in one plane. Each has an aspect ratio of 6.4 and an area of 361 square inches, which includes the portion inside the fuselage. The NACA 23012 profile is maintained along the entire span.

The fuselage is of circular cross section and was constructed as described in reference 2. Its dimensions are presented in table I. With the shortest tail cone attached, the fuselage is geometrically similar to that of reference 4.

Five interchangeable vertical tails and the horizontal tail were made to the NACA 0009 section (fig. 1). Their dimensions are presented in table II.

TESTS

The wings with dihedral angles of 0° and 5° were tested alone at angles of yaw of -5° and 5° over an angle-of-attack range from -10° to 20°. The model combinations tested are shown in table III. Model combinations were tested at angles of yaw of -5°, 0°, and 5° over an angle-of-attack range from -10° to 20° and at an angle of attack of 10.2° over an angle-of-yaw range from -30° to 12°.

All tests were run at a dynamic pressure of 65 pounds per square foot, which corresponds to a test Reynolds number of approximately 388,000 based on an 8-inch wing chord. The data may have been affected by compressibility at large angles of attack.

PRESENTATION OF DATA

The results of the tests are presented in standard NACA coefficients of forces and moments. Rolling-moment and yawing-moment coefficients are given about the center-of-gravity location shown in figure 1. The data are referred to a system of axes in which the Z-axis is in the plane of symmetry and perpendicular to the relative wind, the X-axis is in the plane of symmetry and perpendicular to the Z-axis, and the Y-axis is perpendicular to the plane of symmetry.

The coefficients and symbols used are defined as follows:

C_L lift coefficient (L/qS_w)

C_D drag coefficient (D/qS_w)

C_Y lateral-force coefficient (Y/qS_w)

C_{Y_ψ} slope of curve of lateral-force coefficient against angle of yaw $(\partial C_Y/\partial\psi)$

C_l rolling-moment coefficient (L'/qbS_w)

Cl_ψ slope of curve of rolling-moment coefficient against angle of yaw $\left(\partial C_l/\partial\psi\right)$

C_n yawing-moment coefficient $\left(N/qbS_w\right)$

Cn_ψ slope of curve of yawing-moment coefficient against angle of yaw $\left(\partial C_n/\partial\psi\right)$

Δ_1 increment of Cn_ψ or CY_ψ caused by wing-fuselage interference

Δ_2 increment of Cn_ψ or CY_ψ caused by wing-fuselage interference on vertical tail

$\frac{lS_v}{bS_w}$ tail-volume coefficient

D force along X-axis; positive when directed downstream

Y force along Y-axis; positive when directed to the right

L force along Z-axis; positive when directed upward

N yawing moment about Z-axis; positive when tends to retard right wing

L' rolling moment about X-axis; positive when tends to depress right wing

q dynamic pressure $\left(\frac{1}{2}\rho V^2\right)$

V free-stream velocity

ρ mass density of air

S_w wing area (2.507 sq ft)

b wing span (4 ft)

Γ dihedral angle, degrees

l tail length; measured from center of gravity, which is assumed to be 10.40 inches behind nose of model on center line of fuselage, to hinge line of tail surfaces

S_v vertical-tail area

α angle of attack, degrees

ψ angle of yaw, degrees

The static-lateral-stability slopes Cn_ψ, Cl_ψ, and CY_ψ were obtained from data measured at $\psi = \pm 5^\circ$ since the yaw tests showed that the coefficients had an approximately linear variation in the range of angle of yaw from 5° to -5°. In order to indicate the validity of this procedure, the slopes obtained from yaw tests at $\psi = 0^\circ$ are plotted with tailed symbols in the figures.

The accuracy of Cn, Cl, and CY was determined experimentally to be about ± 0.0005, ± 0.0008, and ± 0.001, respectively. The average experimental accuracy of Cn_ψ, Cl_ψ, and CY_ψ is about ± 0.00010, ± 0.00016, and ± 0.0002, respectively. The accuracies of the angle-of-attack and angle-of-yaw measurements are about 0.1° and 0.05°, respectively.

Angle of attack and drag coefficient were corrected for tunnel-wall effect by the following formulas:

$$\Delta\alpha = 57.3\delta_w \frac{S_w}{C} C_L = 0.609 C_L \quad \text{(deg)}$$

$$\Delta C_D = \delta_w \frac{S_w}{C} C_L^2 = 0.0106 C_L^2$$

where

δ_w jet-boundary correction factor at wing (0.1525)

C cross-sectional area of tunnel (36 sq ft)

Both corrections are additive. No jet-boundary corrections were applied to C_l, C_n, and C_Y. The correction to C_Y is within the experimental error, whereas the corrections to C_n and C_l would be subtractive and equal to about 1 percent.

The C_L and C_D data were corrected for the support-strut effect; no corrections were applied to C_Y, C_l, or C_n since previous results indicated the magnitude of these corrections to be small for this model and support system.

The values of Δ_1 and Δ_2 for C_{n_ψ} for the model without wing fillets were obtained by the following formulas:

$$\Delta_1 C_{n_\psi} = C_{n_\psi}{}_{\text{wing-fuselage combination}} - \left(C_{n_\psi}{}_{\text{wing}} + C_{n_\psi}{}_{\text{fuselage}}\right)$$

$$\Delta_2 C_{n_\psi} = C_{n_\psi}{}_{\text{complete model}} - \left(C_{n_\psi}{}_{\text{wing}} + C_{n_\psi}{}_{\text{fuselage with hor. and vert. tails on}} + \Delta_1 C_{n_\psi}\right)$$

The values of Δ_1 and Δ_2 for C_{Y_ψ} may be obtained in the same manner. The method used in this investigation to obtain Δ_1 and Δ_2 is the same as that of reference 5. The following formula (by which the value of C_{n_ψ} for the complete model is obtained) is an example of the application of the increments Δ_1 and Δ_2:

$$C_{n_\psi} = C_{n_\psi}{}_{\text{wing}} + C_{n_\psi}{}_{\text{fuselage with hor. and vert. tails on}} + \Delta_1 C_{n_\psi} + \Delta_2 C_{n_\psi}$$

The interference between the fuselage and vertical tail and the interference between the fuselage and horizontal tail were not determined.

Lift-coefficient and drag-coefficient data for representative model configurations are shown in figure 3. The lateral-stability slopes C_{n_ψ} and C_{Y_ψ} for the wing

are presented in figure 4. The data presented in the figures are summarized in table IV.

DISCUSSION

For the complete model, the static-lateral-stability slopes C_{n_ψ} and C_{Y_ψ} usually decreased with a positive increase in angle of attack (figs. 12 and 15). The results of the present investigation indicate that this decrease was caused by interference (figs. 5 and 6). With the vertical tail off, the variation of these values with angle of attack was irregular apparently also because of interference (figs. 9 and 11). Such variations with α of the lateral-stability slopes as were obtained in the present investigation for the low-wing model both with and without a vertical tail were not shown in the midwing investigation (reference 3). The slopes C_{Y_ψ} and C_{n_ψ} were practically always greater for the low-wing than for the midwing configuration, apparently because of a change in interference with wing location.

At negative and sometimes at small positive angles of attack, C_{l_ψ} decreased as the angle of attack became less negative (figs. 12 and 15). In the positive angle-of-attack range, C_{l_ψ} generally increased with angle of attack. The slope C_{l_ψ} was increased because of the side force on the vertical tail at negative and small positive angles of attack but the opposite was true at large positive angles of attack. This effect may be attributed to the system of axes used. For this system of axes, the center of pressure of the vertical tail is above the X-axis at negative and small positive angles of attack; consequently the side force on the vertical tail caused a positive increment of C_{l_ψ}. The opposite was true at large positive angles of attack because the center of pressure was below the X-axis. The slope C_{l_ψ} was appreciably greater for the midwing configuration than for the low-wing configuration, frequently by as much as 3° of effective dihedral (reference 3). This change in slope is evidently caused by a change in the nature of the flow around the wing near the wing-fuselage juncture.

Interference Effects

The increments caused by wing-fuselage interference Δ_1 and by wing-fuselage interference on the vertical tail Δ_2 were computed by the equations previously given. The fuselage data (with and without tail surfaces) used in these computations were taken from reference 2. The other data were obtained from the present investigation.

The quantities $\Delta_1 C_{n_\psi}$ and $\Delta_1 C_{Y_\psi}$ were generally appreciable and had a stabilizing effect on the model (fig. 5). The variation of these values with angle of attack was irregular, but $\Delta_1 C_{Y_\psi}$ generally tended to decrease with a positive increase in angle of attack. The irregularity of the curves may be caused by a burble at the juncture of the wing and fuselage, additional evidence of which may be seen in the curves of lift and drag coefficients in figure 3. An appreciable part of the value of C_{Y_ψ} for the wing-fuselage combination can be attributed to interference. The changes in $\Delta_1 C_{n_\psi}$ and $\Delta_1 C_{Y_\psi}$ with fuselage length were within the experimental accuracy for the fuselage lengths tested.

At negative and small positive angles of attack, the quantities $\Delta_2 C_{n_\psi}$ and $\Delta_2 C_{Y_\psi}$ were generally appreciable and had a stabilizing effect on the model (fig. 6). With an additional positive increase in angle of attack, the values changed in such a manner as to become destabilizing. The effect of replacing vertical tail 2 by vertical tail 4 (a 48-percent increase in area) on these quantities was generally small in the unstalled range. The variations of $\Delta_2 C_{n_\psi}$ and $\Delta_2 C_{Y_\psi}$ with fuselage length were somewhat irregular. Because the model tested in this investigation had no wing fillet, caution should be used in applying the results to design since the presence of a fillet may appreciably change the lateral stability characteristics. In view of this fact, an investigation of the lateral stability characteristics of a model with wing fillets might be desirable.

Effect of Horizontal Tail

Theory indicates that the presence of the horizontal tail would increase the effective aspect ratio of the vertical tail and thus increase C_{n_ψ} and C_{Y_ψ}. A small increase in these quantities was obtained by the addition of the horizontal tail (figs. 7 and 8). This increment varied somewhat irregularly with angle of attack. A comparison with the results of reference 3 showed that the end-plate effect was greater for the midwing configuration. Data from reference 5 indicate that this difference is due to a change in the wing-fuselage interference on the vertical tail with wing location. In reference 3 an incremental increase of 0.0010 in C_{Y_ψ} was computed for the end-plate effect of the horizontal tail on vertical tail 4. An average increase of 0.0005 was obtained from the present experimental investigation. The end-plate effect of the horizontal tail on C_{l_ψ} amounted to less than 1° of effective dihedral. The results of the present investigation (fig. 8) indicate that, although separation begins to occur on the vertical tail at about the same time with the horizontal tail on and off, it progresses more rapidly with the horizontal tail on.

With the vertical tail off, the magnitude of the static-lateral-stability slopes was not appreciably affected by the addition of the horizontal tail (figs. 9 and 11).

Effect of Changes in Fuselage Length

Within the scope of the present investigation, a slight increase in C_{n_ψ} was generally obtained with a longer fuselage for the model having no vertical tail (figs. 9 to 11). The effect was more pronounced at the larger negative angles of attack.

For the complete model equipped with vertical tail 4, the increase in C_{n_ψ} with fuselage length was approximately linear (figs. 12 and 13). This increment of C_{n_ψ}, which resulted from increased fuselage length, appreciably diminished with a positive increase in angle of attack. This decrease may be partly caused by interference. A comparison with the results of reference 3 showed that,

for the midwing configuration, the increase of C_{n_ψ} with fuselage length was also linear but remained fairly constant with a change in angle of attack.

The variations of C_{l_ψ} and C_{Y_ψ} were small, for the fuselage lengths tested, both with and without a vertical tail. A similar result was obtained for the midwing configuration (reference 3).

Effect of Changes in Vertical-Tail Area

The slopes C_{n_ψ} and C_{Y_ψ} increased approximately linearly with vertical-tail area (figs. 14 to 17). The rate of change of C_{n_ψ} with vertical-tail area was greatest in a small region between angles of attack of -4° and 0° and decreased as the angle of attack varied from this range. This change in vertical-tail effectiveness with angle of attack might be attributed to interference. For the midwing configuration, the increases in these slopes with vertical-tail area were also approximately linear and fairly constant over the unstalled angle-of-attack range (reference 3).

As would be expected, at negative and small positive angles of attack, C_{l_ψ} increased with vertical-tail area whereas, at large positive angles of attack, the opposite was true. A similar result was obtained for the midwing configuration (reference 3).

Effect of Changes with Constant Tail Volume

In figures 18 and 19 the result of changing the fuselage length and vertical-tail area in such a manner as to hold the tail volume constant is shown. The configurations in which the tail volume remained constant are shown in table V. Data from figures 18 and 19 are cross-plotted in figure 14. The vertical tails tested all had an aspect ratio of 2.15.

The slope C_{n_ψ} should remain approximately the same with constant tail volume. The experimental variation is small over the normal flight range and may be partly caused by interference or might be explained by the arbitrary manner in which the tail-volume coefficient was defined.

The values of Cl_ψ and CY_ψ are dependent mainly on tail area and are practically independent of tail length (fig. 14). For the range of variations giving constant tail volume, the changes in both CY_ψ and Cl_ψ were appreciable.

Effects of Changes in Dihedral

For the model having no vertical tail, the change in Cn_ψ with dihedral angle was small (figs. 9 to 11). With the vertical tail on, Cn_ψ was slightly larger for $\Gamma = 0^\circ$ than for $\Gamma = 5^\circ$ (figs. 12 to 17). Similar trends were also obtained for the midwing configuration (reference 3). Figure 14 shows that increased dihedral angle slightly decreased the rate of change of Cn_ψ with vertical-tail area but had a negligible effect on the rate of change of Cn_ψ with fuselage length. The slope CY_ψ was generally slightly greater for $\Gamma = 0^\circ$ than for $\Gamma = 5^\circ$ except at large positive angles of attack.

The changes with dihedral angle of wing-fuselage interference and wing-fuselage interference on the vertical tail were small.

Comparison of Data from Langley 7- by 10-Foot and Langley Stability Tunnels

The model tested in the Langley stability tunnel is 0.8 as large and geometrically similar to the one tested in the Langley 7- by 10-foot tunnel for the investigation of reference 4. The test Reynolds number, based on the wing chord, was about 619,000 for the Langley 7- by 10-foot tunnel compared with about 888,000 for the Langley stability tunnel. The effective Reynolds number, however, was about the same since the turbulence factor for the Langley 7- by 10-foot tunnel is 1.6, compared with less than 1.1 for the Langley stability tunnel. Data taken from reference 4 were converted to the stability axes and the angle of attack was corrected for tunnel-wall effect in order to make the data comparable with data from the Langley stability tunnel. Figure 20 shows

that satisfactory agreement was obtained, in general, for all three static-lateral-stability slopes. In both tunnels the stall occurred at about the same angle of attack and the model, when yawed, tended to roll violently at the stall.

CONCLUSIONS

The results of tests of a model consisting of a rectangular low wing on a circular fuselage with variations in vertical-tail area and fuselage length with and without a horizontal tail indicated, for the range of configurations tested, the following conclusions:

1. The influence of wing-fuselage interference on the slope of the curve of yawing-moment coefficient against angle of yaw C_{n_ψ} and the slope of the curve of lateral-force coefficient against angle of yaw C_{Y_ψ} was usually stabilizing, appreciable, and varied with angle of attack. The effect of wing-fuselage interference on the values of C_{n_ψ} and C_{Y_ψ} contributed by the vertical tail was also generally stabilizing and appreciable at negative and small positive angles of attack but varied with angle of attack.

2. The end-plate effect of the horizontal tail slightly increased the efficiency of the vertical tail. The experimental increment obtained was only one-half the computed value.

3. Increasing the fuselage length with no vertical tail resulted in a slight increase in C_{n_ψ} for the model, both with and without a horizontal tail. At the larger negative angles of attack, the effect was more pronounced. For the complete model, the increase in C_{n_ψ} was approximately linear with fuselage length. The magnitude of the increase appreciably diminished with a positive increase in angle of attack. The changes in the slope of the curve of rolling-moment coefficient against yaw C_{l_ψ} and in C_{Y_ψ} with fuselage length were small.

4. The slopes C_{n_ψ} and C_{Y_ψ} increased approximately linearly with vertical-tail area. For the system of axes used, C_{l_ψ} increased with vertical-tail area at negative and small positive angles of attack but the opposite was true at large positive angles of attack.

5. Increased dihedral angle slightly decreased the rate of change of C_{n_ψ} with vertical-tail area but had a negligible effect on the rate of change of C_{n_ψ} with fuselage length. Except at large positive angles of attack, C_{Y_ψ} was greater with the smaller dihedral angle.

Langley Memorial Aeronautical Laboratory
National Advisory Committee for Aeronautics
Langley Field, Va.

REFERENCES

1. Zimmerman, Charles H.: An analysis of Lateral Stability in Power-Off Flight with Charts for Use in Design. NACA Rep. No. 589, 1937.

2. Fehlner, Leo F., and MacLachlan, Robert: Investigation of Effect of Sideslip on Lateral Stability Characteristics. I - Circular Fuselage with Variations in Vertical-Tail Area and Tail Length with and without Horizontal Tail Surface. NACA ARR No. L4L25, 1944.

3. Hollingworth, Thomas A.: Investigation of Effect of Sideslip on Lateral Stability Characteristics. II - Rectangular Midwing on Circular Fuselage with Variations in Vertical-Tail Area and Fuselage Length with and without Horizontal Tail Surface. NACA ARR No. L5C13, 1945.

4. Bamber, M. J., and House, R. O.: Wind-Tunnel Investigation of Effect of Yaw on Lateral-Stability Characteristics. II - Rectangular N.A.C.A. 23012 Wing with a Circular Fuselage and a Fin. NACA TN No. 730, 1939.

5. Wallace, Arthur R., and Turner, Thomas R.: Wind-Tunnel Investigation of Effect of Yaw on Lateral-Stability Characteristics. V - Symmetrically Tapered Wing with a Circular Fuselage Having a Horizontal and a Vertical Tail. NACA ARR No. 3F23, 1943.

TABLE I

FUSELAGE DIMENSIONS

Fuselage	Fuselage length (in.)	Tail-cone length (in.)	Tail length, l (in.)	$\frac{\text{Tail length}}{\text{Wing span}}$, $\frac{l}{b}$
Short	32.25	9.85	20.07	0.418
Medium	37.05	14.65	24.87	.518
Long	41.85	19.45	29.67	.618

TABLE II

TAIL-SURFACE DIMENSIONS

Tail surface	Designation	Vertical-tail area (sq in.) (1)	$\frac{\text{Vertical-tail area}}{\text{Wing area}}$	Aspect ratio
Vertical	1	10.83	0.0300	2.15
Do---	2	23.78	.0659	2.15
Do---	3	28.37	.0786	2.15
Do---	4	35.16	.0974	2.15
Do---	5	46.20	.1280	2.15
Horizontal	----------	64.21	.178	3.99

[1]Area measured from root chord at center line of fuselage.

NATIONAL ADVISORY
COMMITTEE FOR AERONAUTICS

NATIONAL ADVISORY
COMMITTEE FOR AERONAUTICS

TABLE III

MODEL COMBINATIONS TESTED

Horizontal tail	Vertical tail	Fuselage	Dihedral angle (deg)	Variable
On	Off	Short, medium, and long	0 and 5	α
	1			
	2			
	3			
	4			
	5			
	2	Long		ψ
	4			
	3	Medium		
	4			
	4	Short		
Off	Off			α and ψ
	Off	Long		α
	Off		5	ψ
	4	Short	0 and 5	α and ψ

NATIONAL ADVISORY
COMMITTEE FOR AERONAUTICS

TABLE IV

PRESENTATION OF RESULTS

Figure	Description of figure	Data presented
3	Lift and drag curves for representative model configurations	C_L and C_D as f(α)
4	Slope of yawing-moment and lateral-force coefficients for NACA 23012 rectangular wing	Cn_ψ and CY_ψ as f(α)
5	Effect of wing-fuselage interference	$\Delta_1 Cn_\psi$ and $\Delta_1 CY_\psi$ as f(α)
6	Effect of wing-fuselage interference on vertical tail	$\Delta_2 Cn_\psi$ and $\Delta_2 CY_\psi$ as f(α)
7	End-plate effect of horizontal tail	Cn_ψ, Cl_ψ, and CY_ψ as f(α)
8	End-plate effect of horizontal tail	Cn, Cl, and CY as f(ψ)
9	Effect of changing fuselage length (no tail surfaces)	Cn_ψ, Cl_ψ, and CY_ψ as f(α)
10	Effect of changing fuselage length (no tail surfaces)	Cn, Cl, and CY as f(ψ)
11	Effect of changing fuselage length (horizontal tail on; vertical tail off)	Cn_ψ, Cl_ψ, and CY_ψ as f(α)
12	Effect of changing fuselage length (horizontal tail and vertical tail 4 on)	Cn_ψ, Cl_ψ, and CY_ψ as f(α)
13	Effect of changing fuselage length (horizontal tail and vertical tail 4 on)	Cn, Cl, and CY as f(ψ)

TABLE IV - Concluded

PRESENTATION OF RESULTS - Concluded

Figure	Description of figure	Data presented
14	Effect of changing fuselage length	C_{n_ψ}, C_{l_ψ}, and C_{Y_ψ} as $f\left(\frac{S_v}{S_w}\right)$
15	Effect of changing vertical-tail area	C_{n_ψ}, C_{l_ψ}, and C_{Y_ψ} as $f(\alpha)$
16	Increment of slope of yawing-moment coefficient against angle of yaw caused by vertical-tail area	ΔC_{n_ψ} as $f\left(\frac{S_v}{S_w}\right)$
17	Effect of changing vertical-tail area	C_n, C_l, and C_Y as $f(\psi)$
18	Effect of changes with tail volume constant	C_{n_ψ}, C_{l_ψ}, and C_{Y_ψ} as $f(\alpha)$
19	Effect of changes with tail volume constant	C_n, C_l, and C_Y as $f(\psi)$
20	Comparison of data from Langley stability and Langley 7- by 10-foot tunnels	C_{n_ψ}, C_{l_ψ}, and C_{Y_ψ} as $f(\alpha)$

NATIONAL ADVISORY
COMMITTEE FOR AERONAUTICS

TABLE V

MODEL CONFIGURATIONS HAVING CONSTANT TAIL VOLUME

Vertical tail	Fuselage	$\frac{\text{Tail length}}{\text{Wing span}}, \frac{l}{b}$	$\frac{\text{Tail area}}{\text{Wing area}}, \frac{S_v}{S_w}$	Tail-volume coefficient, $\frac{lS_v}{bS_w}$
4	Short	0.418	0.0974	0.0407
3	Medium	.518	.0786	.0407
2	Long	.618	.0659	.0407

NATIONAL ADVISORY
COMMITTEE FOR AERONAUTICS

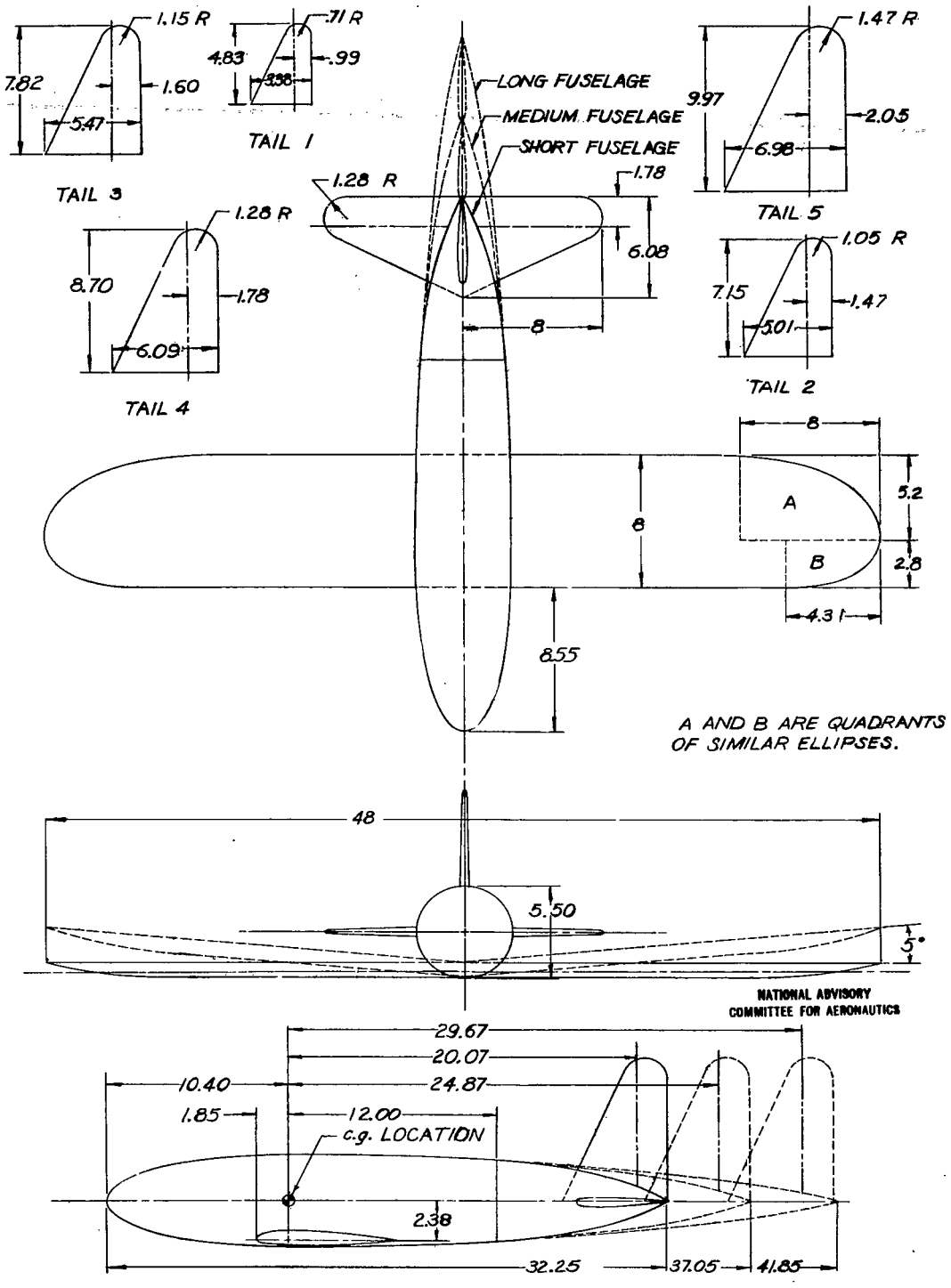

Figure 1.- Rectangular NACA 23012 wing in combination with circular fuselage, vertical and horizontal tails, and tail cones. All dimensions given in inches.

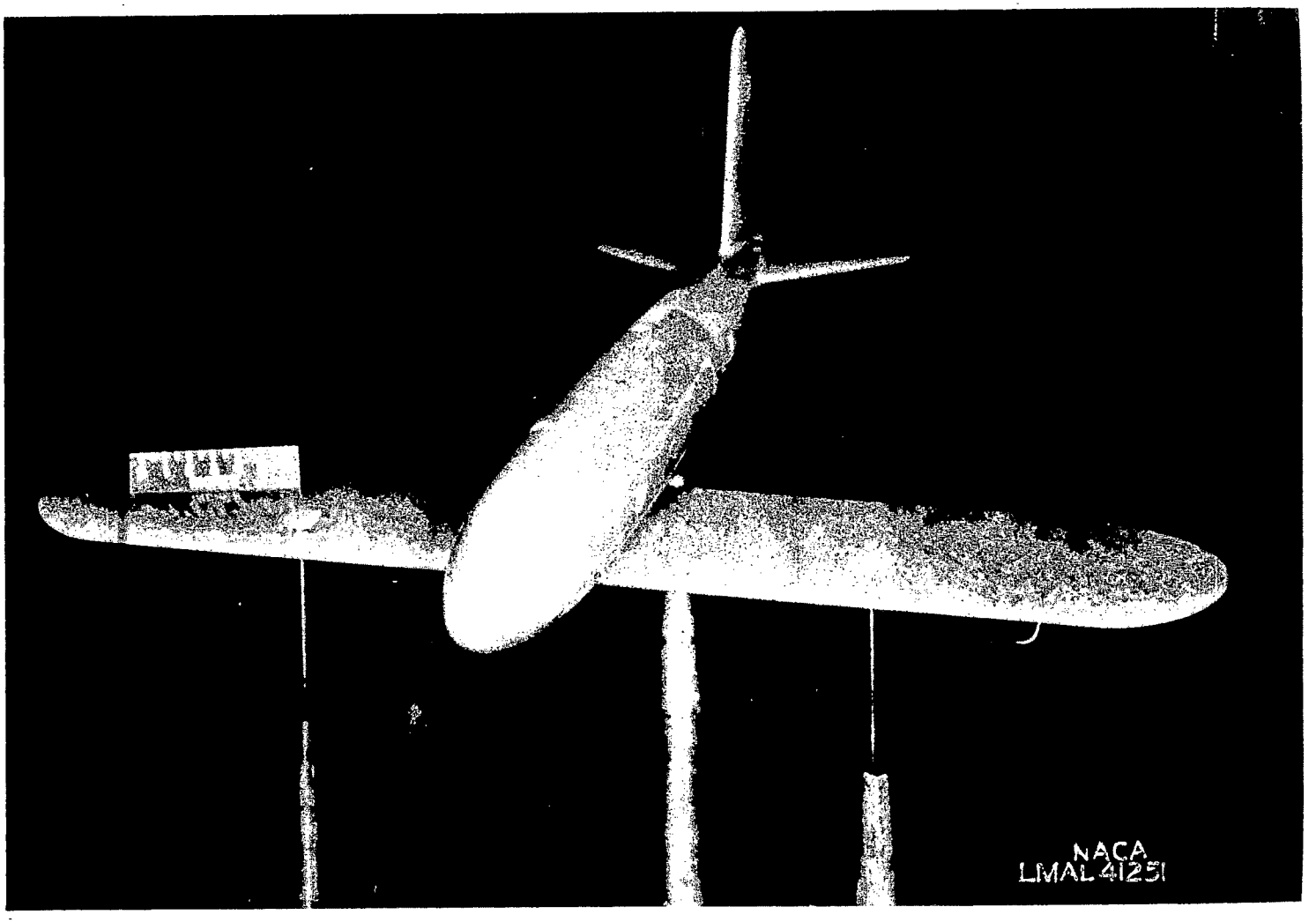

Figure 2.- Rectangular-low-wing model equipped with short fuselage and vertical tail 5 mounted for tests in Langley stability tunnel.

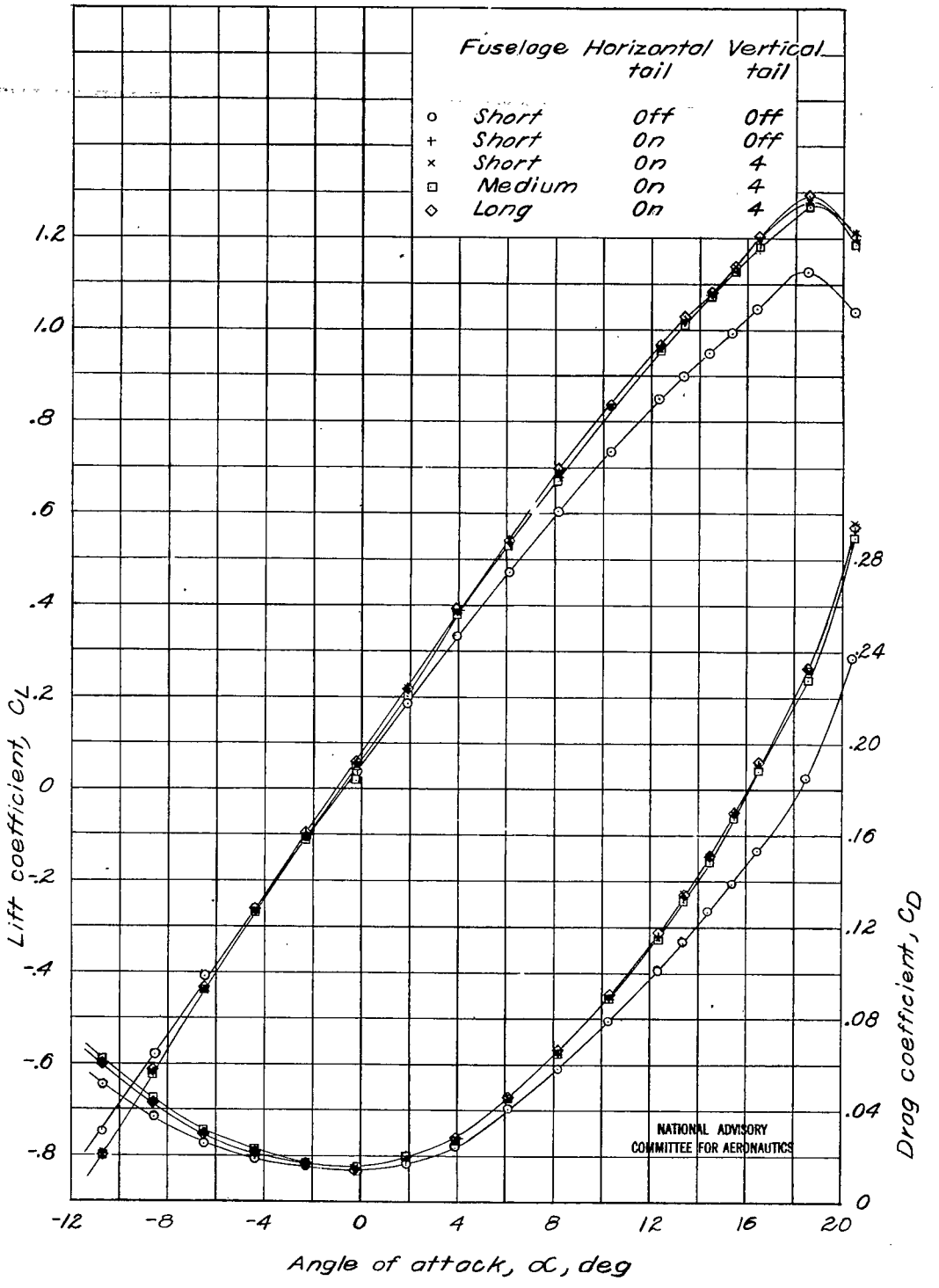

Figure 3.-Variation of lift and drag coefficients with angle of attack for representative model configurations. Γ, 5°; ψ, 0°; q, 65 lb/sq ft.

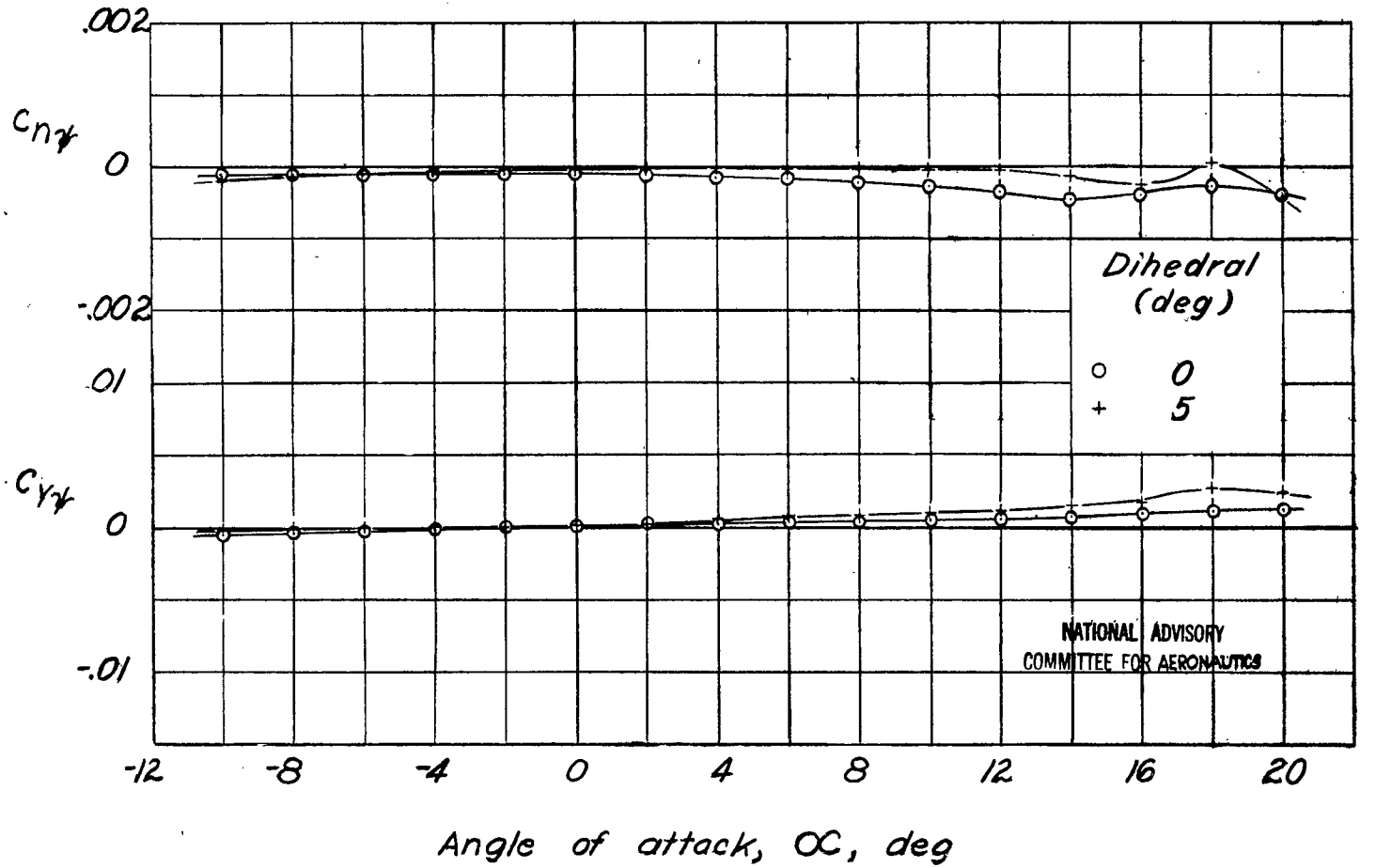

Figure 4.- Variation of lateral-stability slopes C_{n_ψ} and C_{Y_ψ} with angle of attack for NACA 23012 rectangular wing. q, 65 lb/sq ft. (C_{n_ψ} measured about center of gravity.)

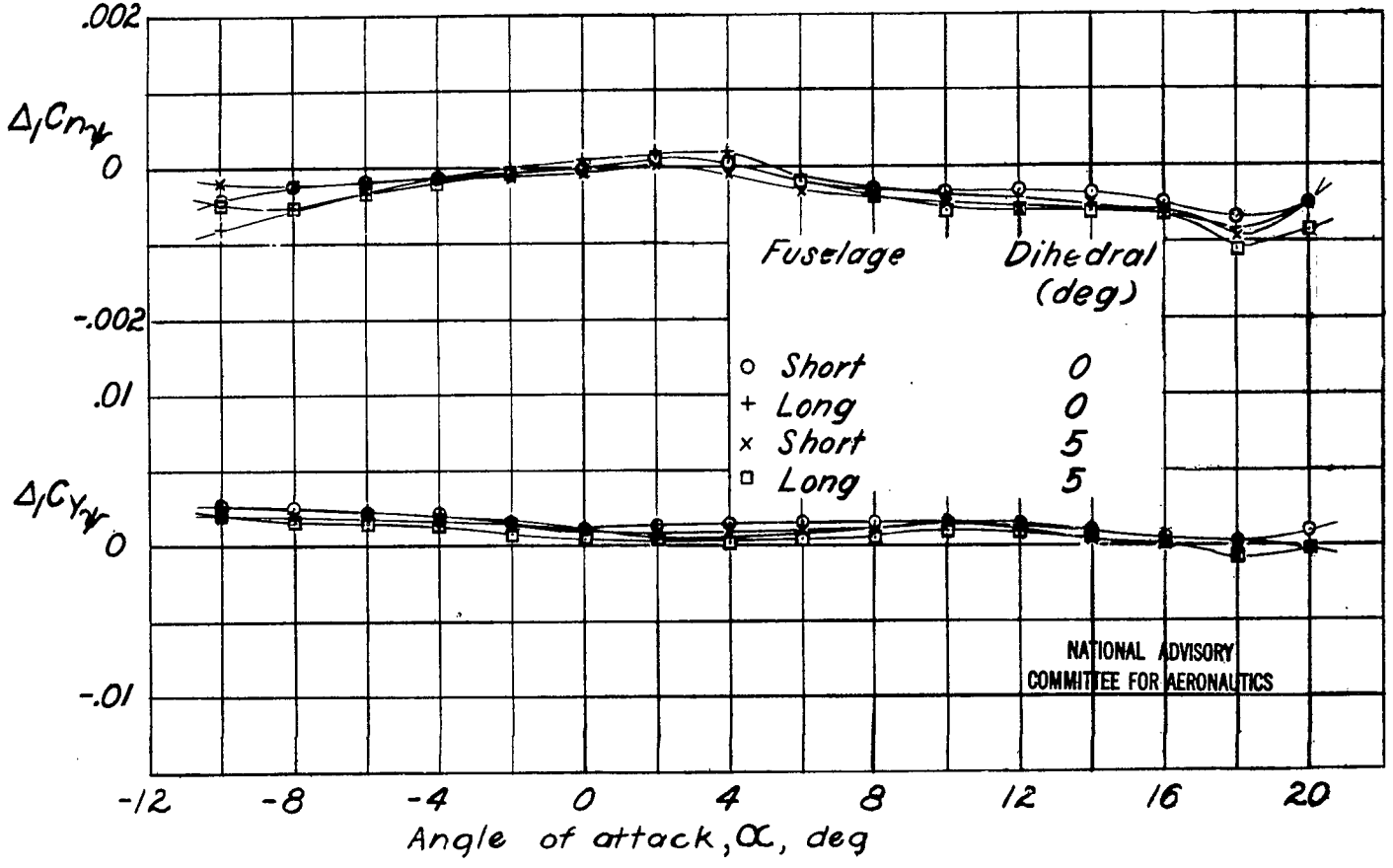

Figure 5.- Increments of C_{n_ψ} and C_{Y_ψ} due to wing-fuselage interference. Horizontal and vertical tails off; q, 65 lb/sq ft.

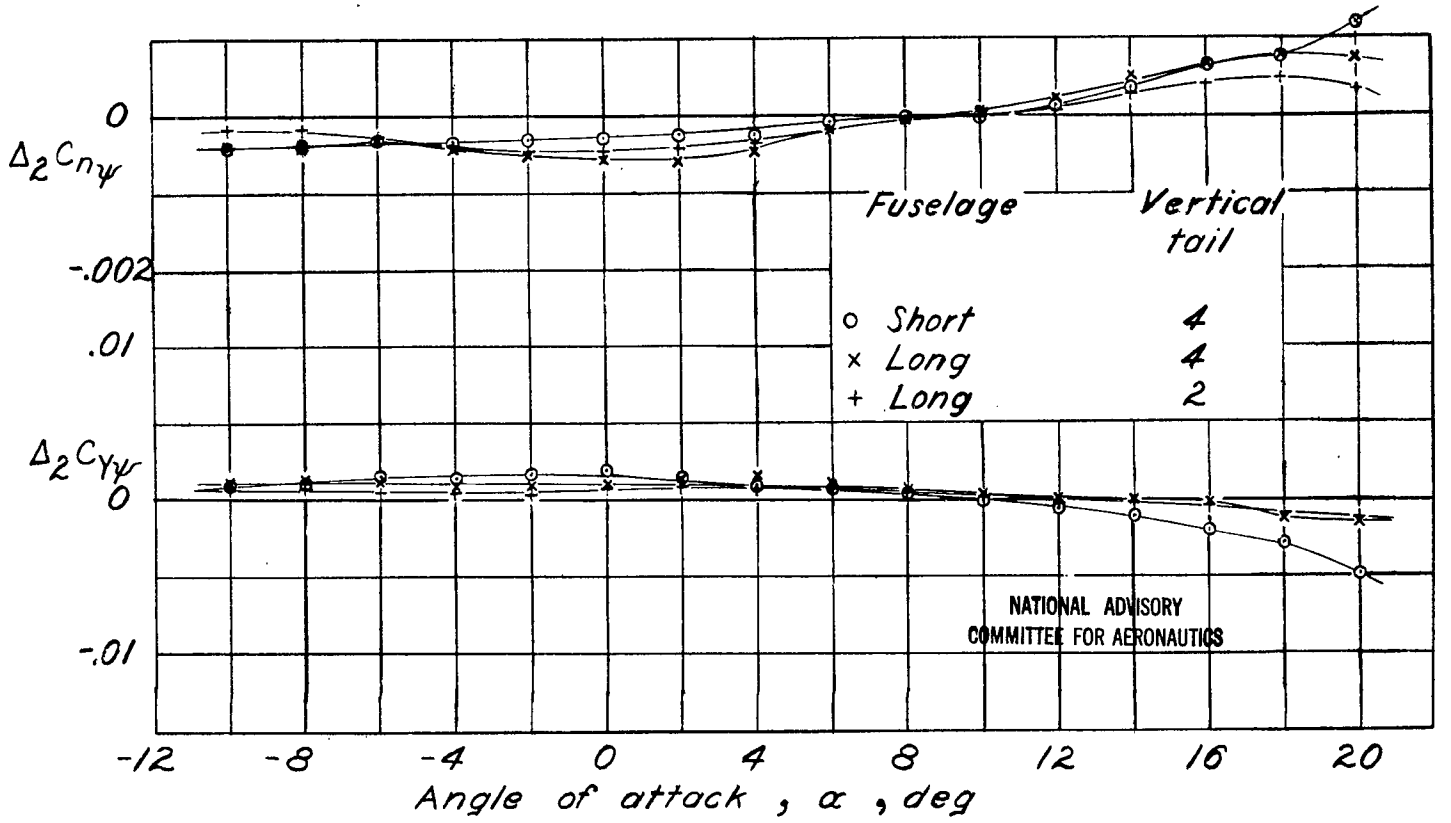

(a) Γ, 0°.

Figure 6.- Increments of C_{n_ψ} and C_{Y_ψ} due to wing-fuselage interference on vertical tail. Horizontal tail on; q, 65 lb/sq ft.

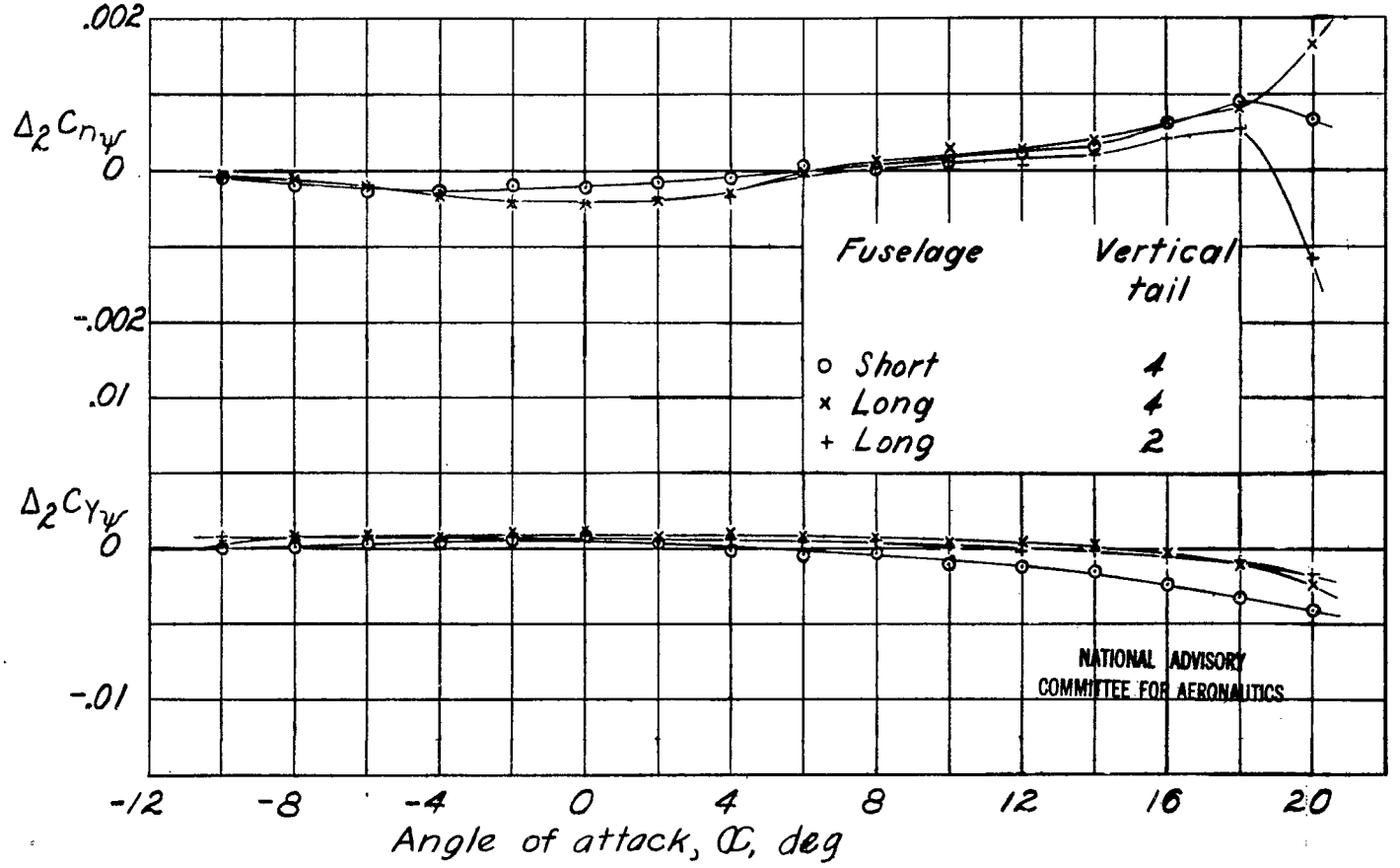

(b) Γ, 5°.

Figure 6.- Concluded.

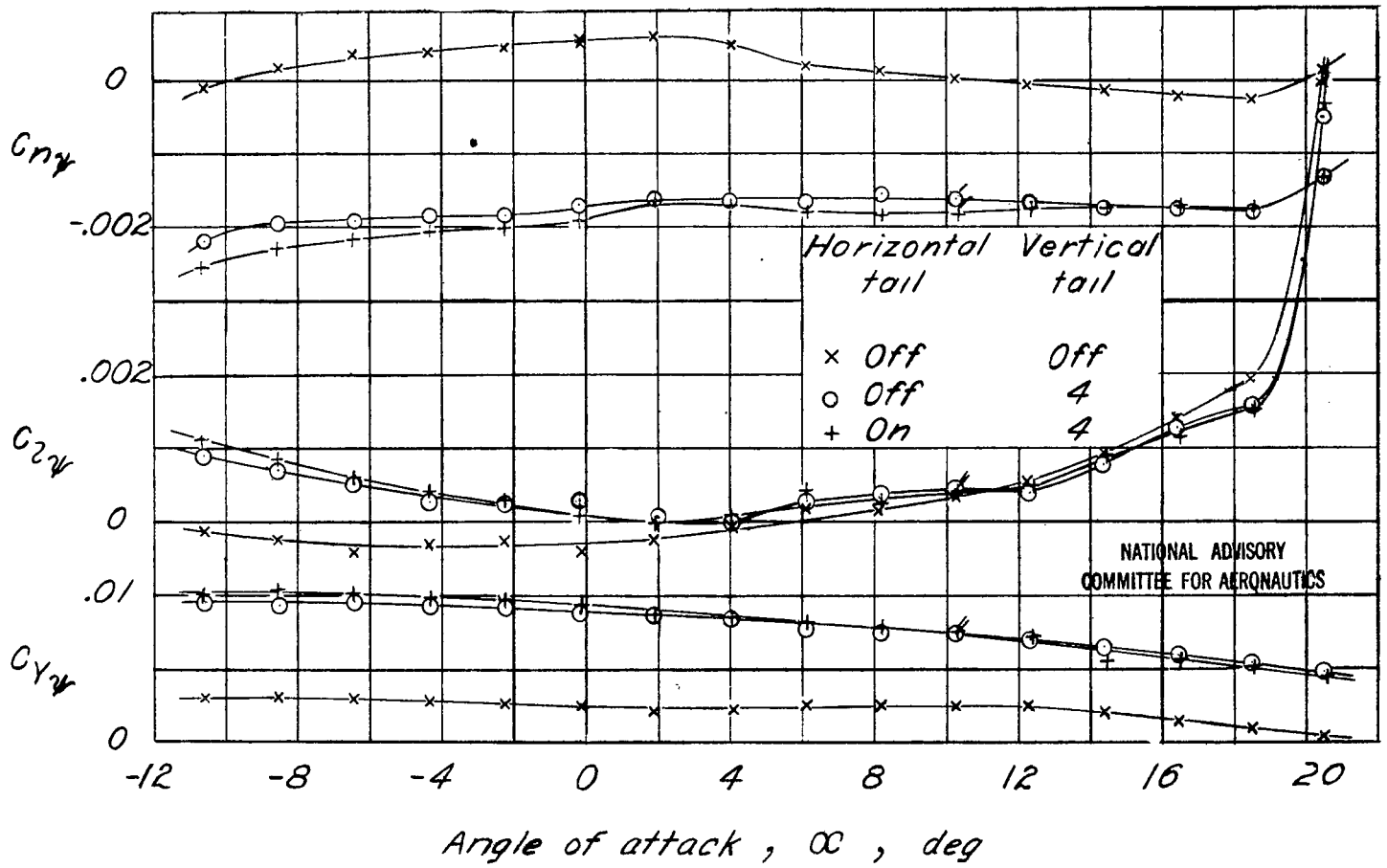

(a) Γ, 0°.

Figure 7.- Effect of horizontal tail surface on variation of lateral-stability slopes C_{n_ψ}, C_{l_ψ}, and C_{Y_ψ} with angle of attack. Short fuselage; q, 65 lb/sq ft.

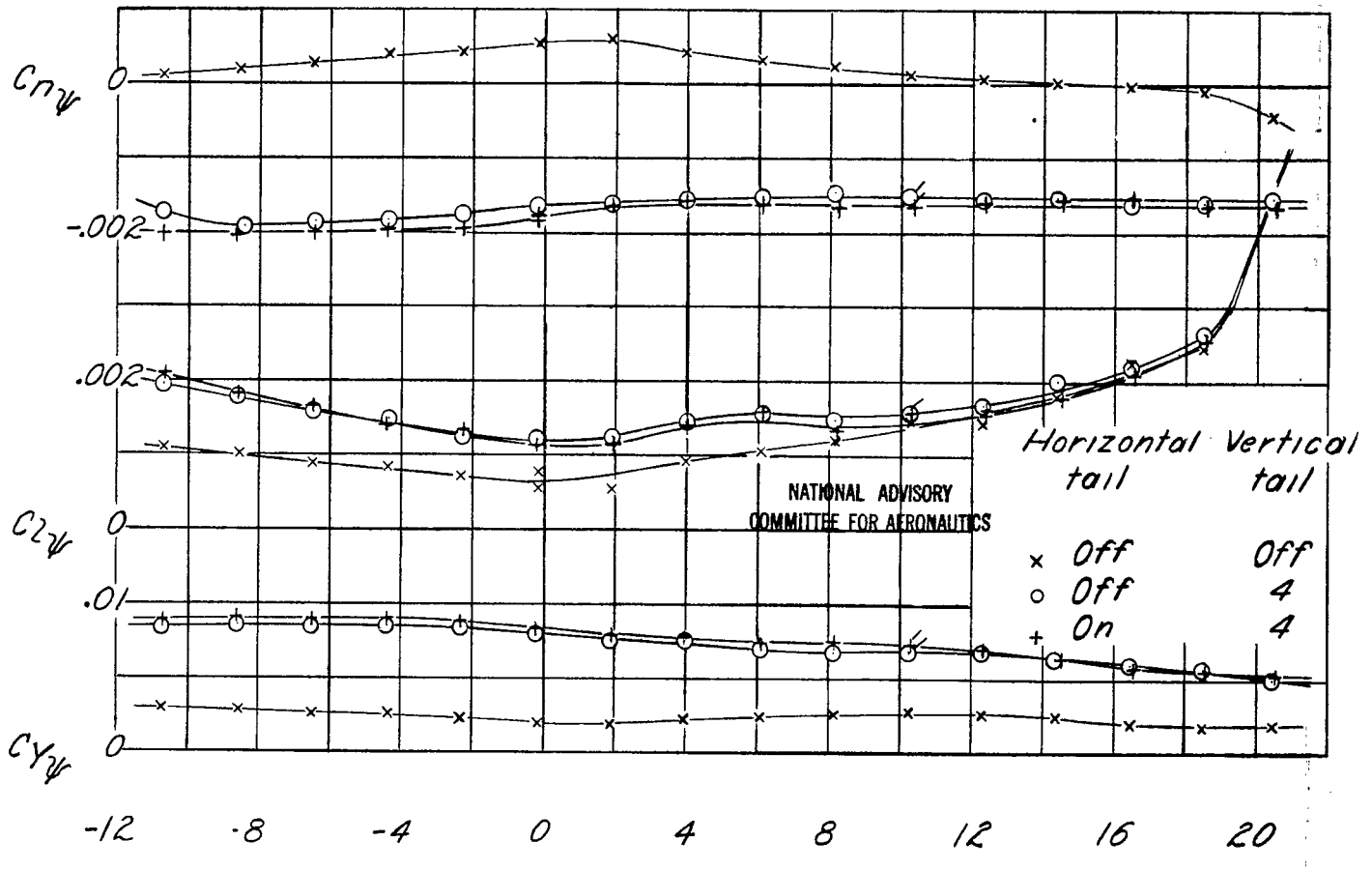

(b) Γ, 5°.

Figure 7.- Concluded.

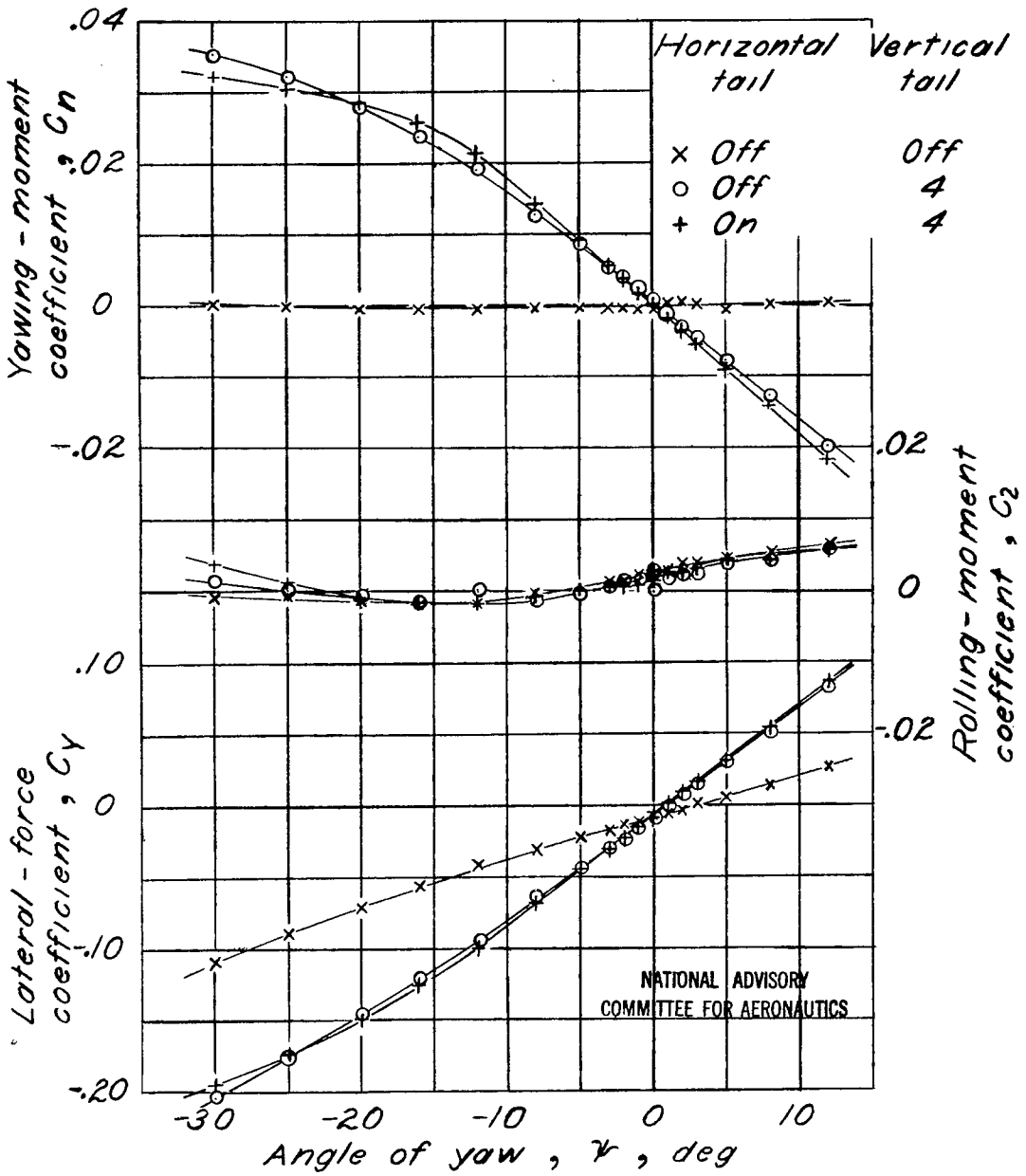

(a) Γ, 0°.

Figure 8. - Effect of horizontal tail surface on variation of yawing-moment, rolling-moment, and lateral-force coefficients with angle of yaw. Short fuselage; α, 10.2°; q, 65 lb/sq ft.

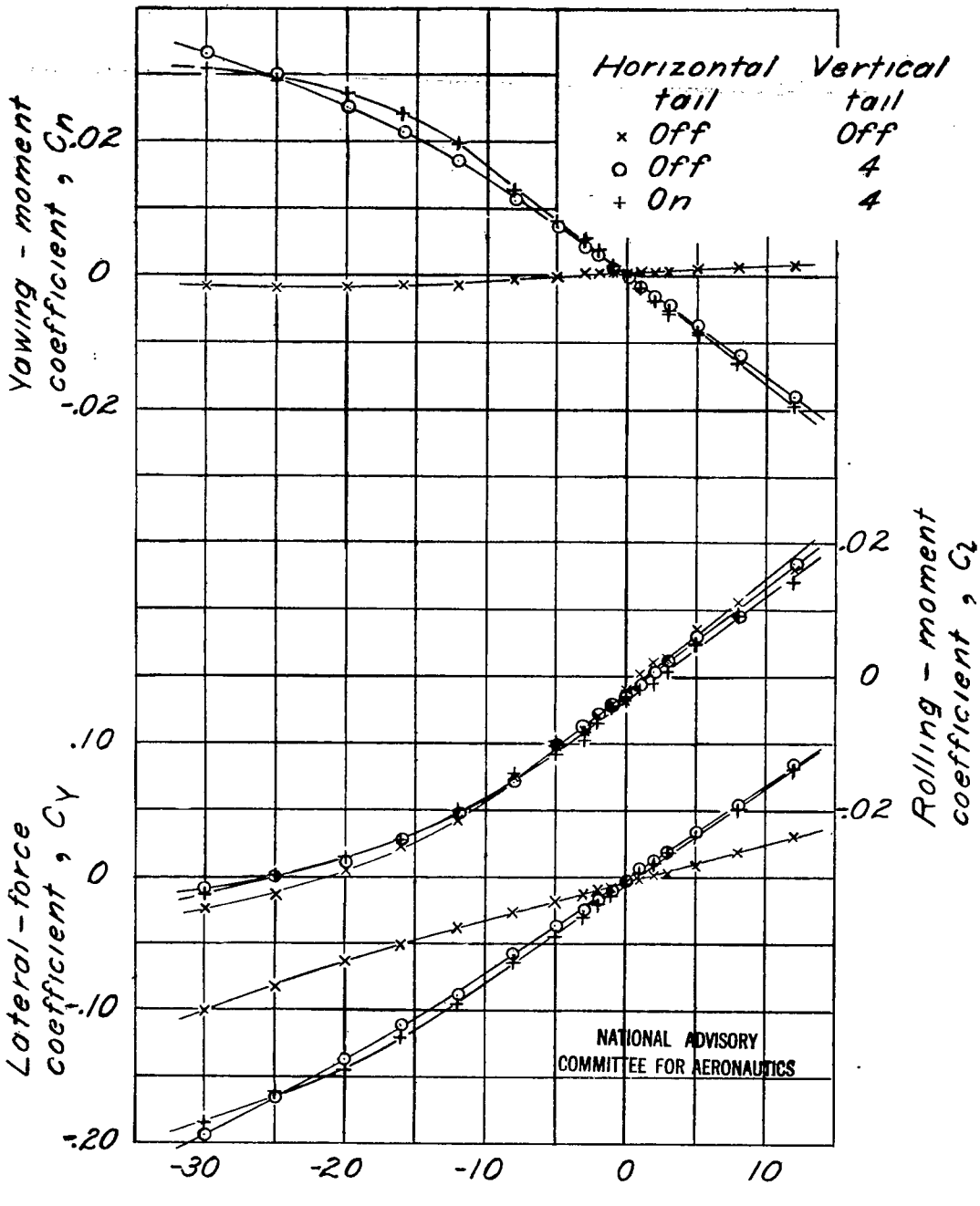

(b) Γ, 5°.

Figure 8. - Concluded.

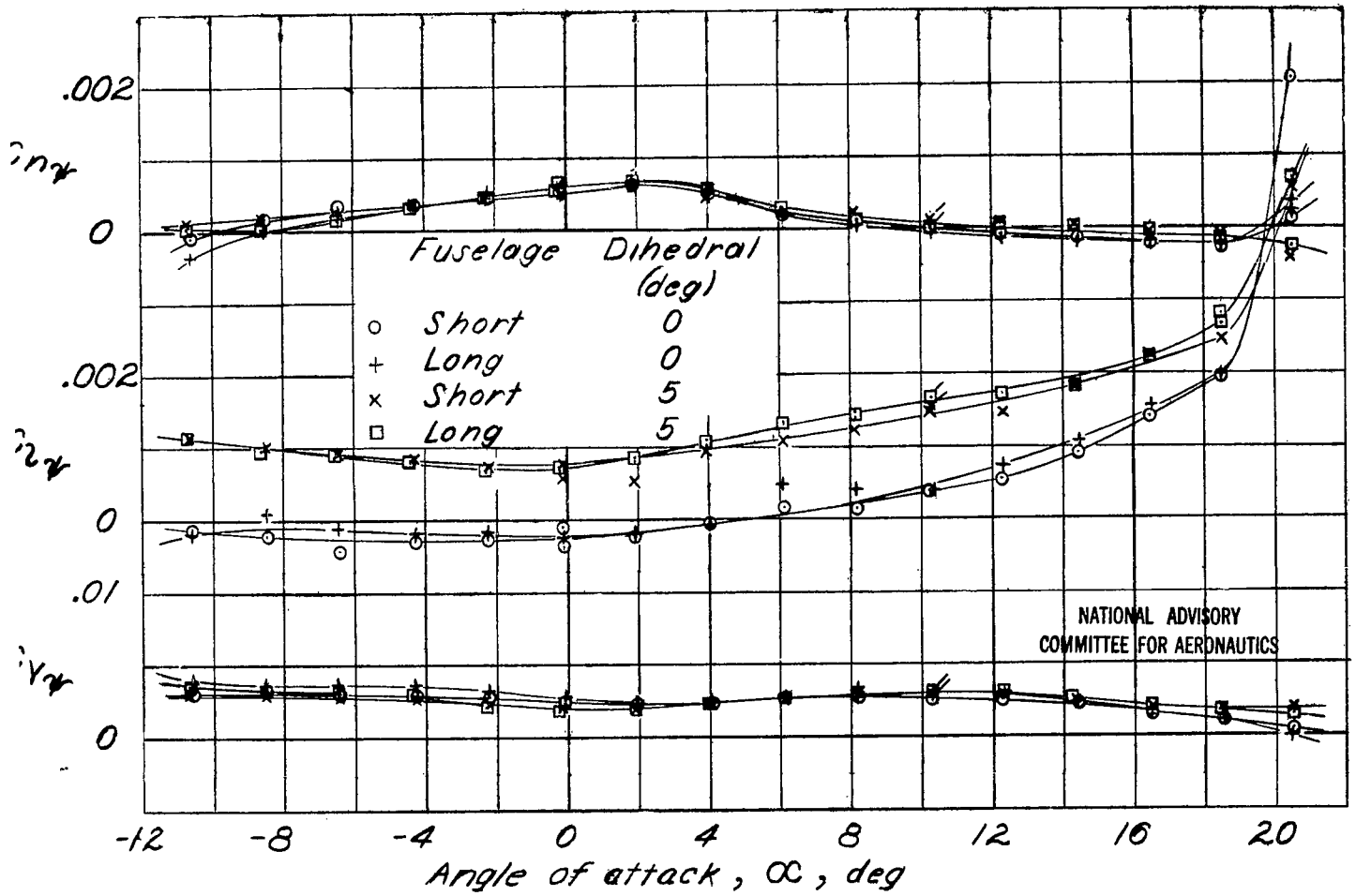

Figure 9.- Effect of changing fuselage length on variation of lateral-stability slopes C_{n_ψ}, C_{l_ψ}, and C_{Y_ψ} with angle of attack. Horizontal and vertical tails off; q, 65 lb/sq ft.

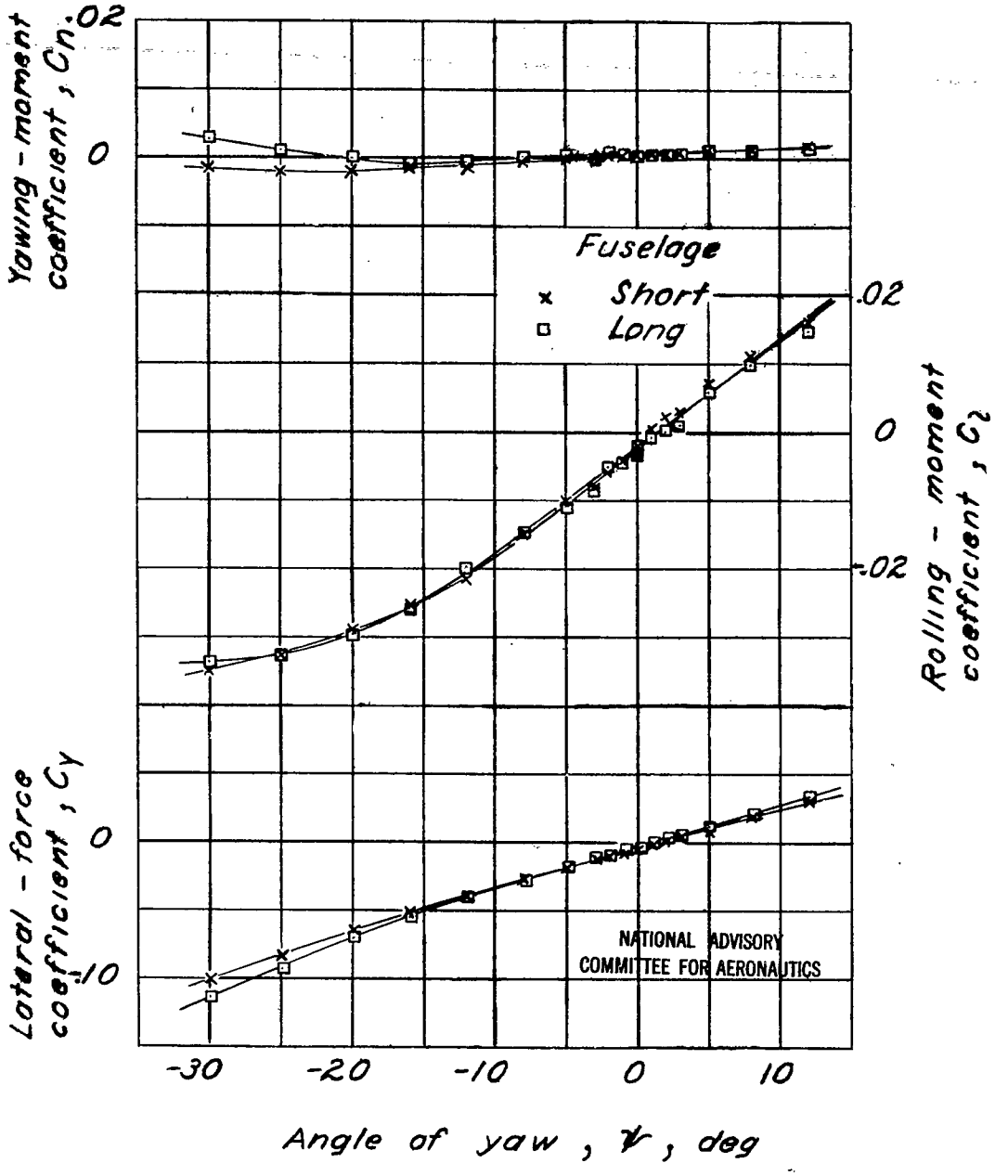

Figure 10 . - Effect of changing fuselage length on variation of yawing - moment , rolling - moment , and lateral - force coefficients with angle of yaw . Horizontal and vertical tails off ; α , 10.2° ; Γ , 5° ; q , 65 lb/sq ft.

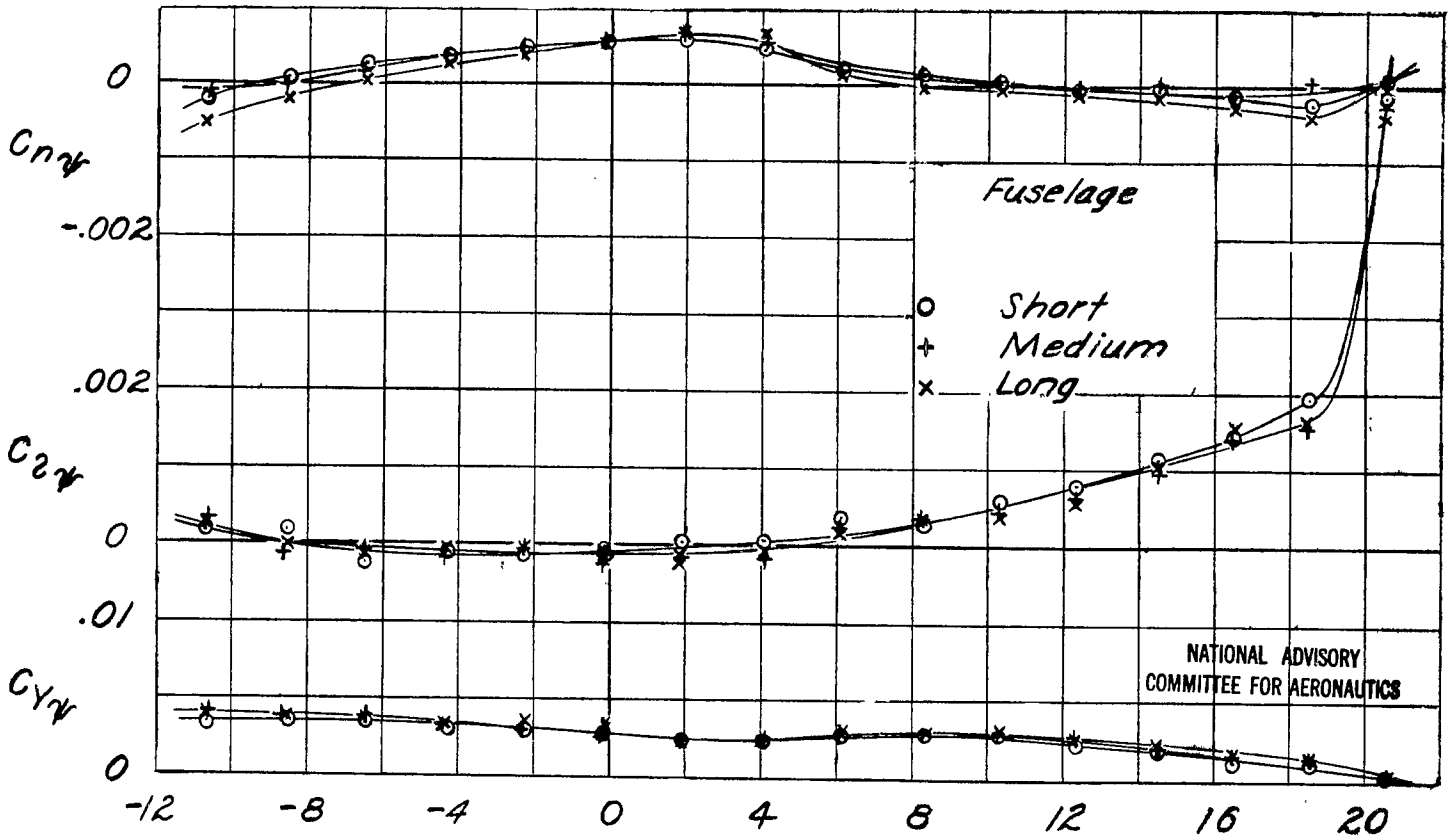

(a) Γ, 0°.

Figure 11.- Effect of changing fuselage length on variation of lateral-stability slopes C_{n_ψ}, C_{l_ψ}, and C_{Y_ψ} with angle of attack. Horizontal tail on; vertical tail off; q, 65 lb/sq ft.

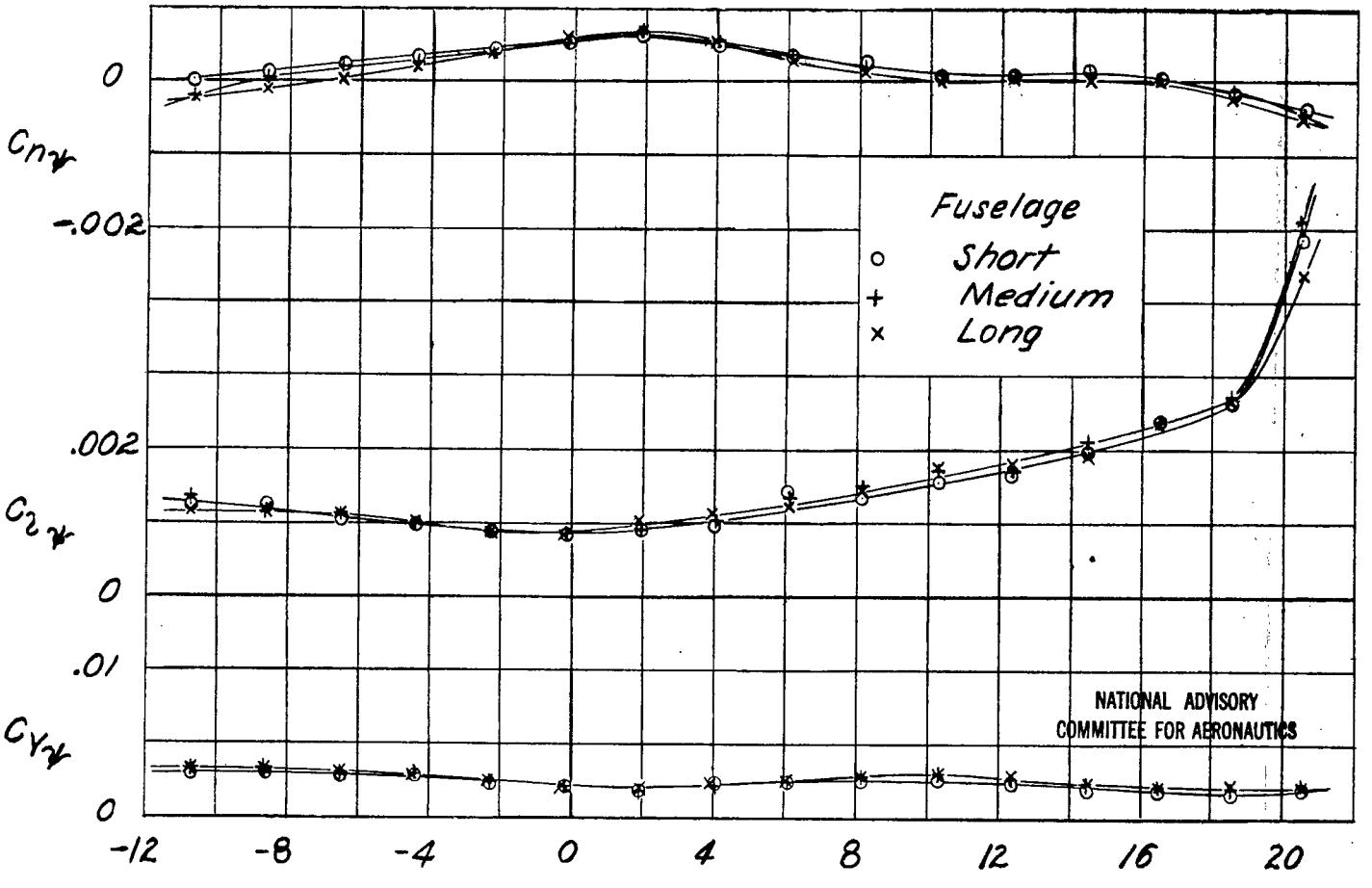

(b) Γ, 5°.

Figure 11.- Concluded.

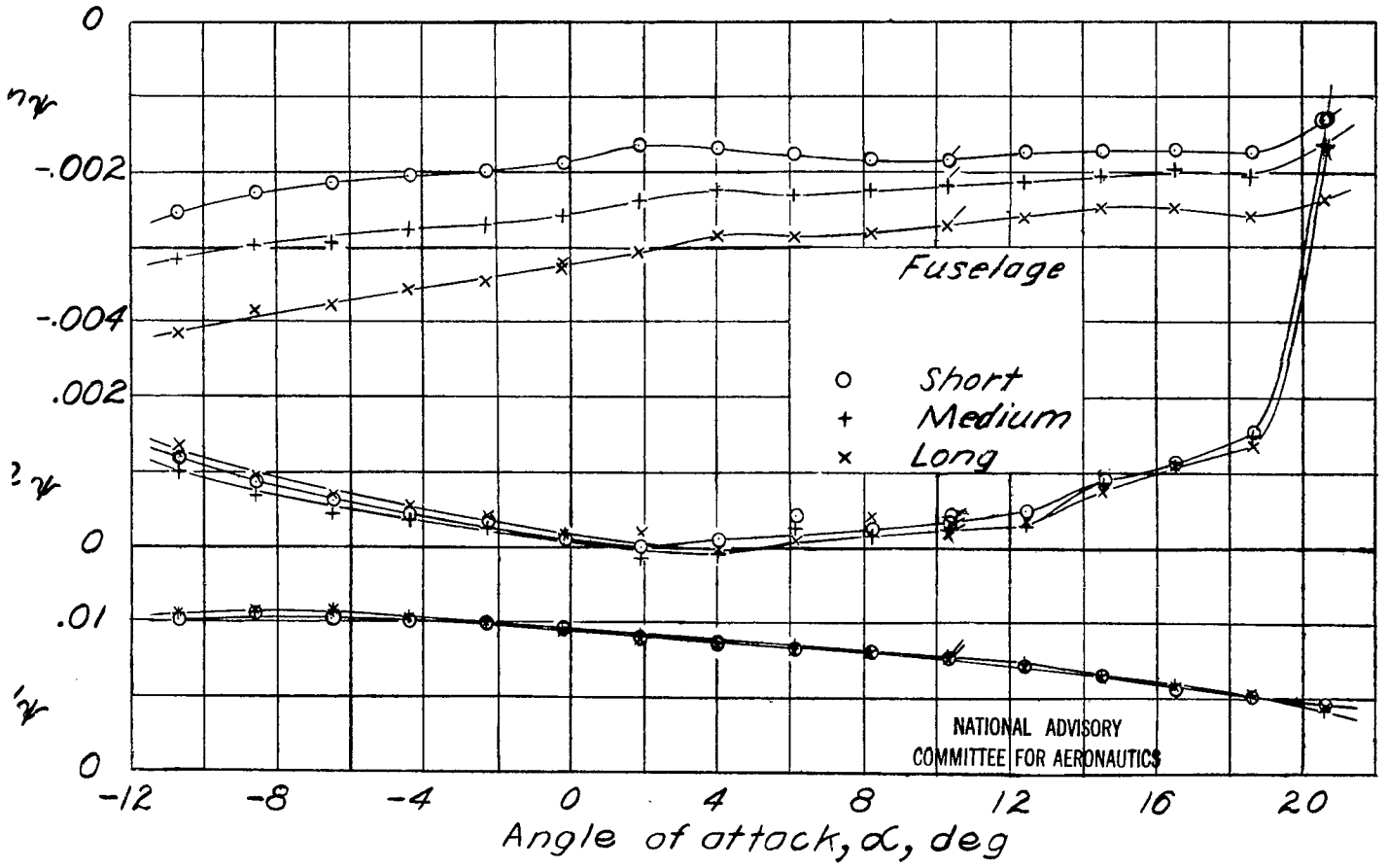

(a) Γ, 0°.

Figure 12.- Effect of changing fuselage length on variation of lateral-stability slopes C_{n_ψ}, C_{l_ψ}, and C_{Y_ψ} with angle of attack. Horizontal tail and vertical tail 4 on ; q , 65 lb/sq ft.

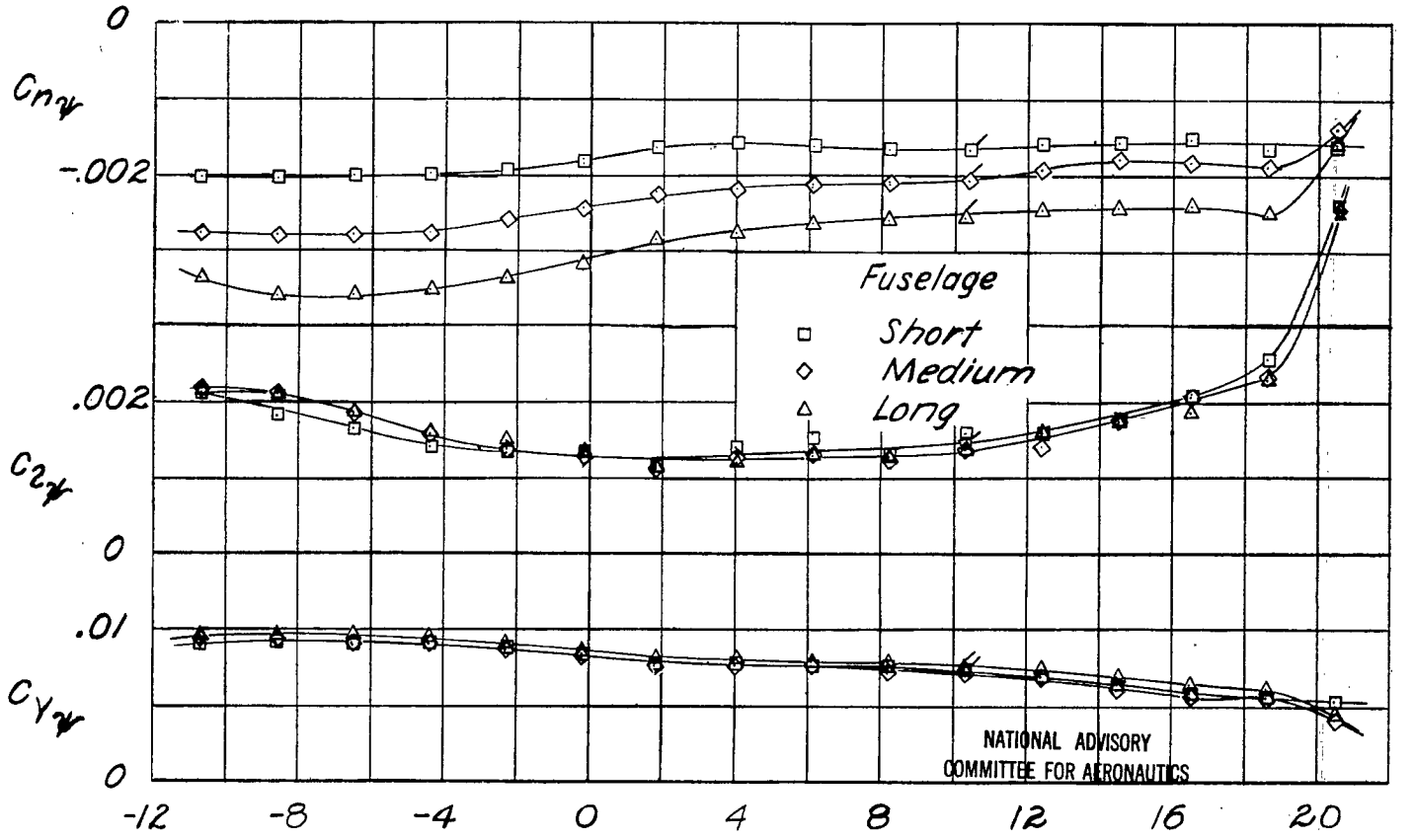

(b) Γ, 5°.

Figure 12.- Concluded.

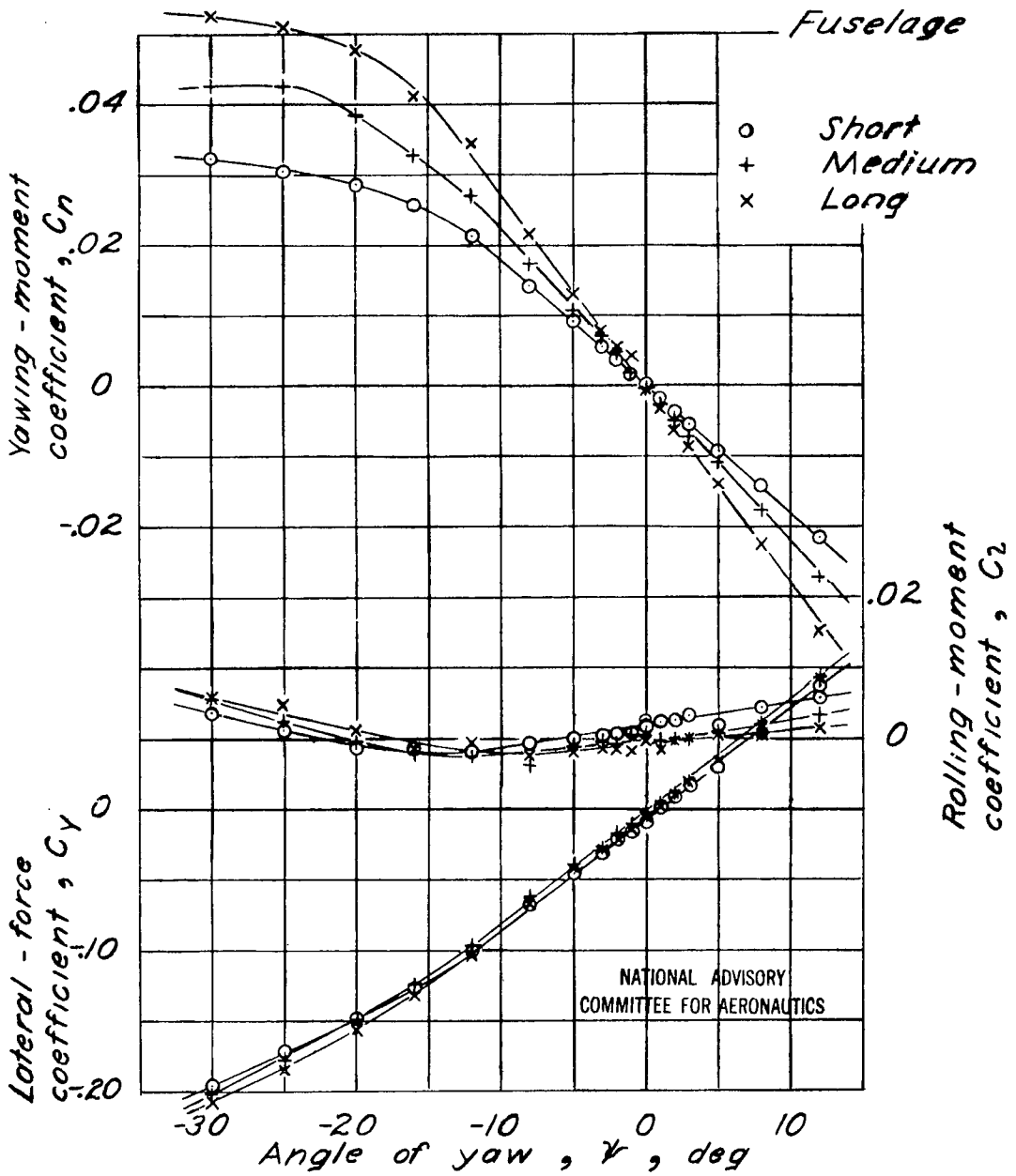

(a) Γ, 0°.

Figure 13.- Effect of fuselage length on variation of yawing-moment, rolling-moment, and lateral-force coefficients with angle of yaw. Horizontal tail and vertical tail 4 on; α, 10.2°; q, 65 lb/sq ft.

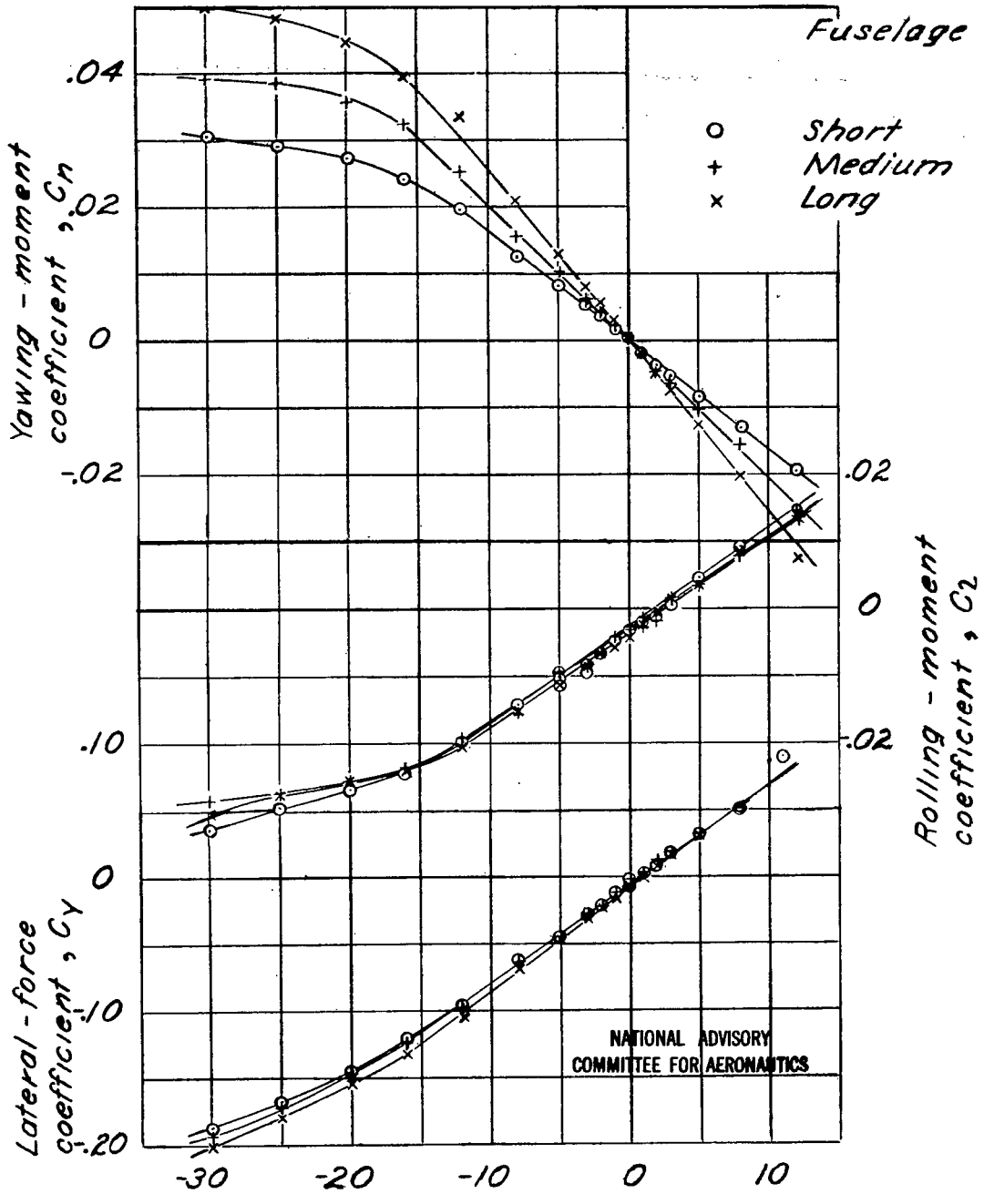

(b) Γ, 5°.

Figure 13. - Concluded.

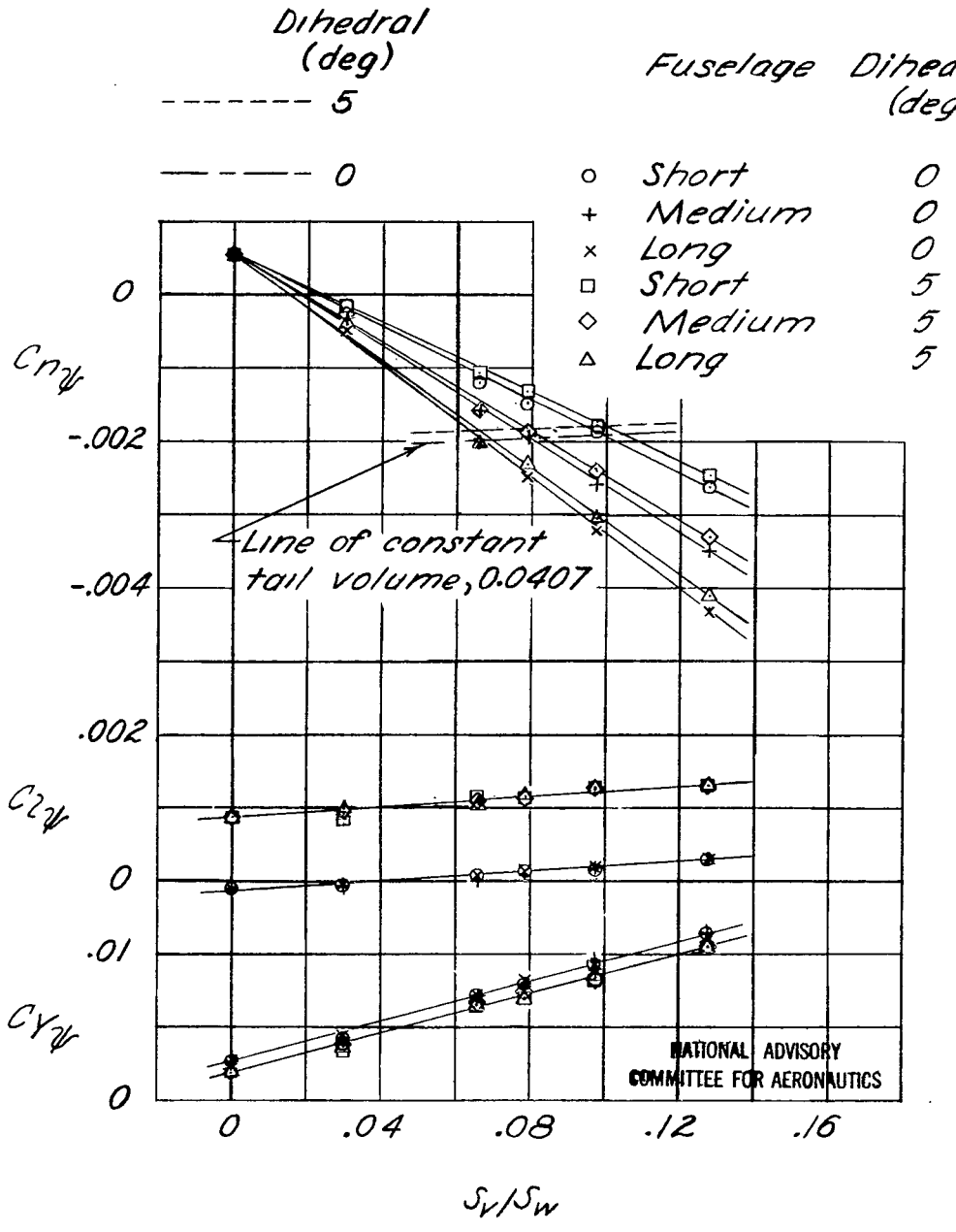

(a) α, 0°.

Figure 14.—Effect of changing fuselage length on variation of lateral-stability slopes C_{n_ψ}, C_{l_ψ}, and C_{Y_ψ} with vertical-tail area. Horizontal tail on ; q, 65 lb/sq ft.

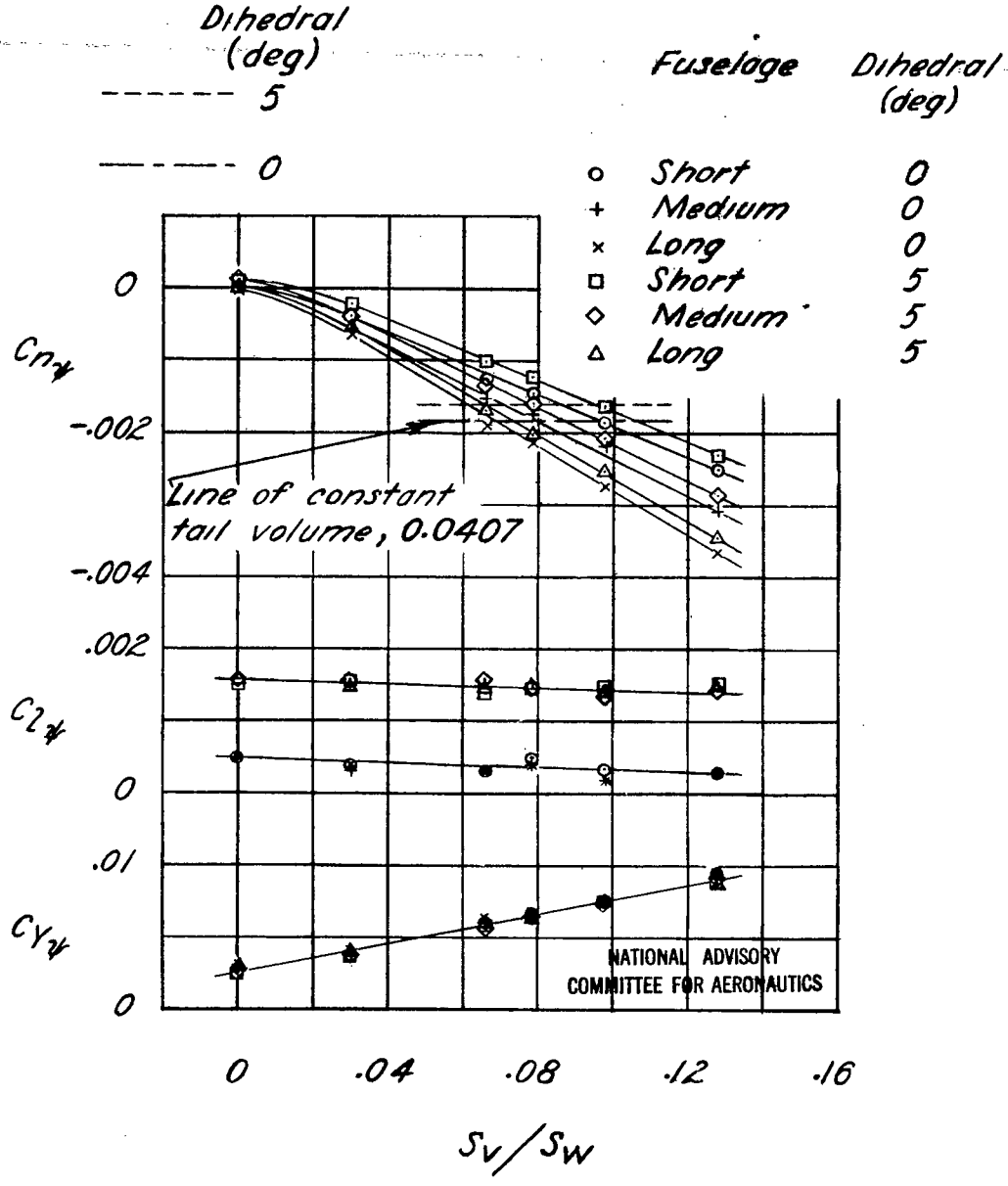

(b) α, 10°.

Figure 14.- Concluded.

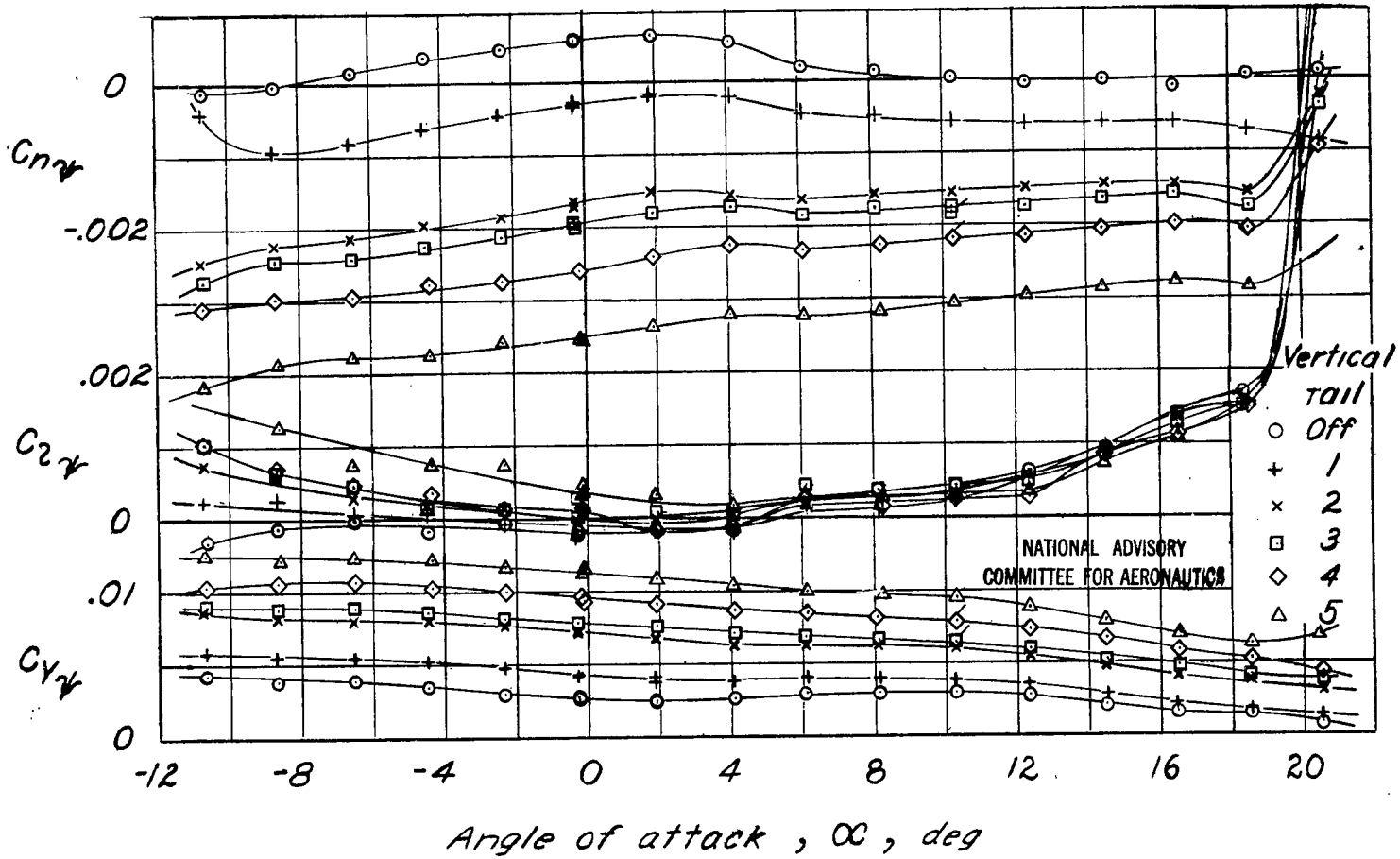

(a) Γ, 0°.

Figure 15.- Effect of changing vertical-tail area on variation of lateral-stability slopes C_{n_ψ}, C_{l_ψ}, and C_{Y_ψ} with angle of attack. Medium-length fuselage with horizontal tail; q, 65 lb/sq ft.

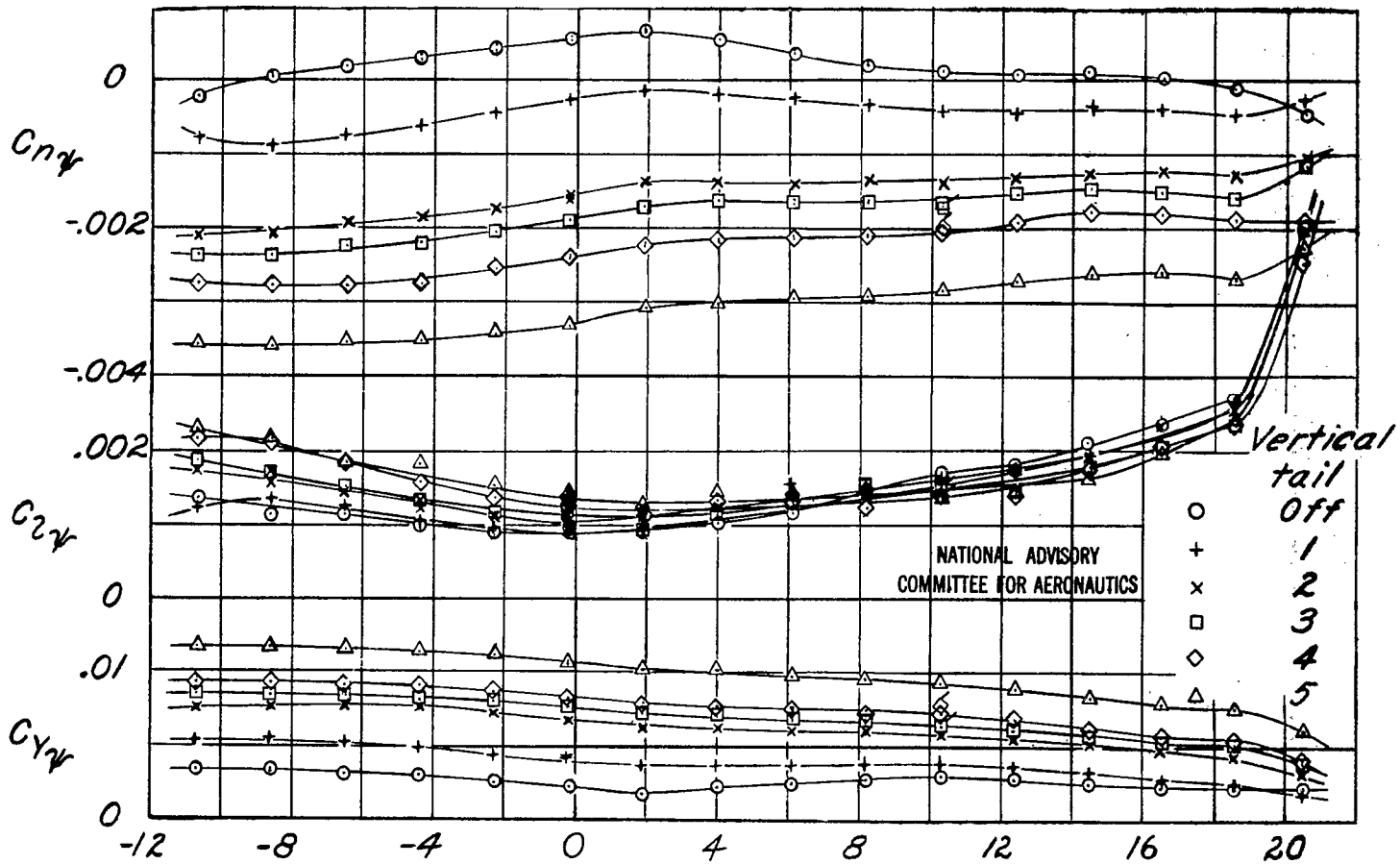

(b) Γ, 5°.

Figure 15.- Concluded.

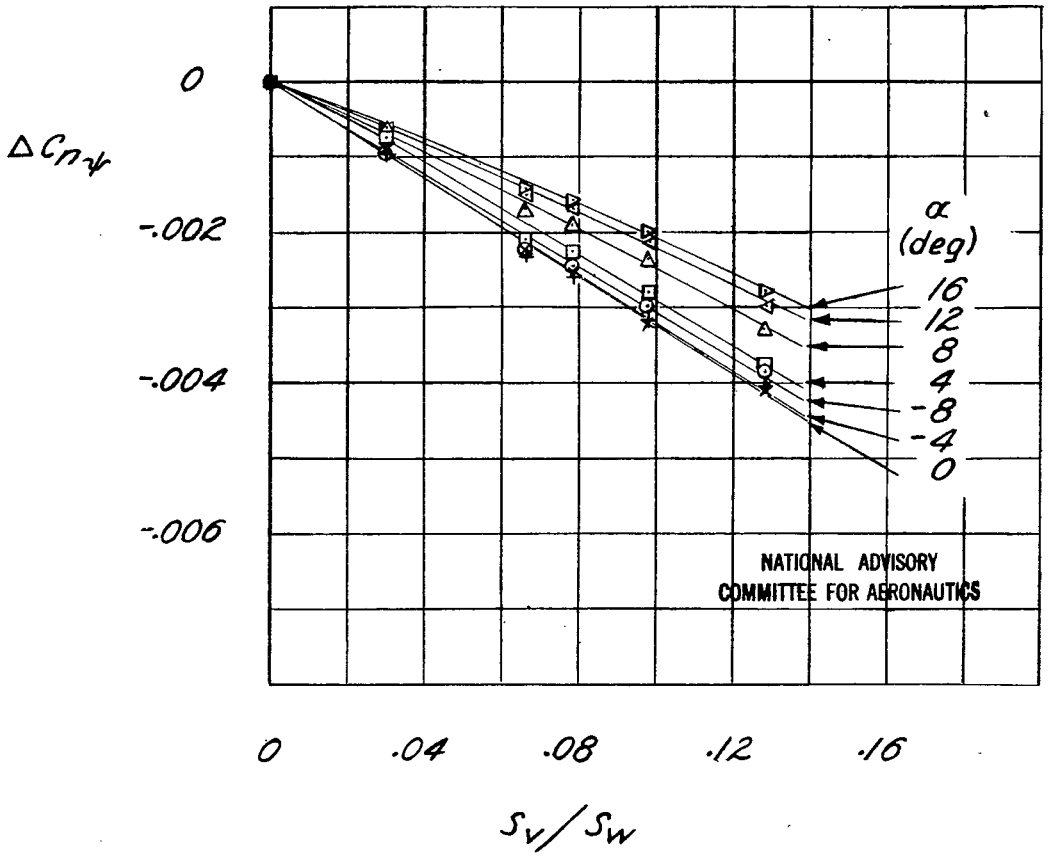

Figure 16.- Increment of lateral-stability slope ΔC_{n_ψ} caused by vertical-tail area. (C_{n_ψ} for medium-length fuselage with horizontal tail and wing with 0° dihedral subtracted from C_{n_ψ} for complete model to obtain ΔC_{n_ψ}.) q, 65 lb/sq ft.

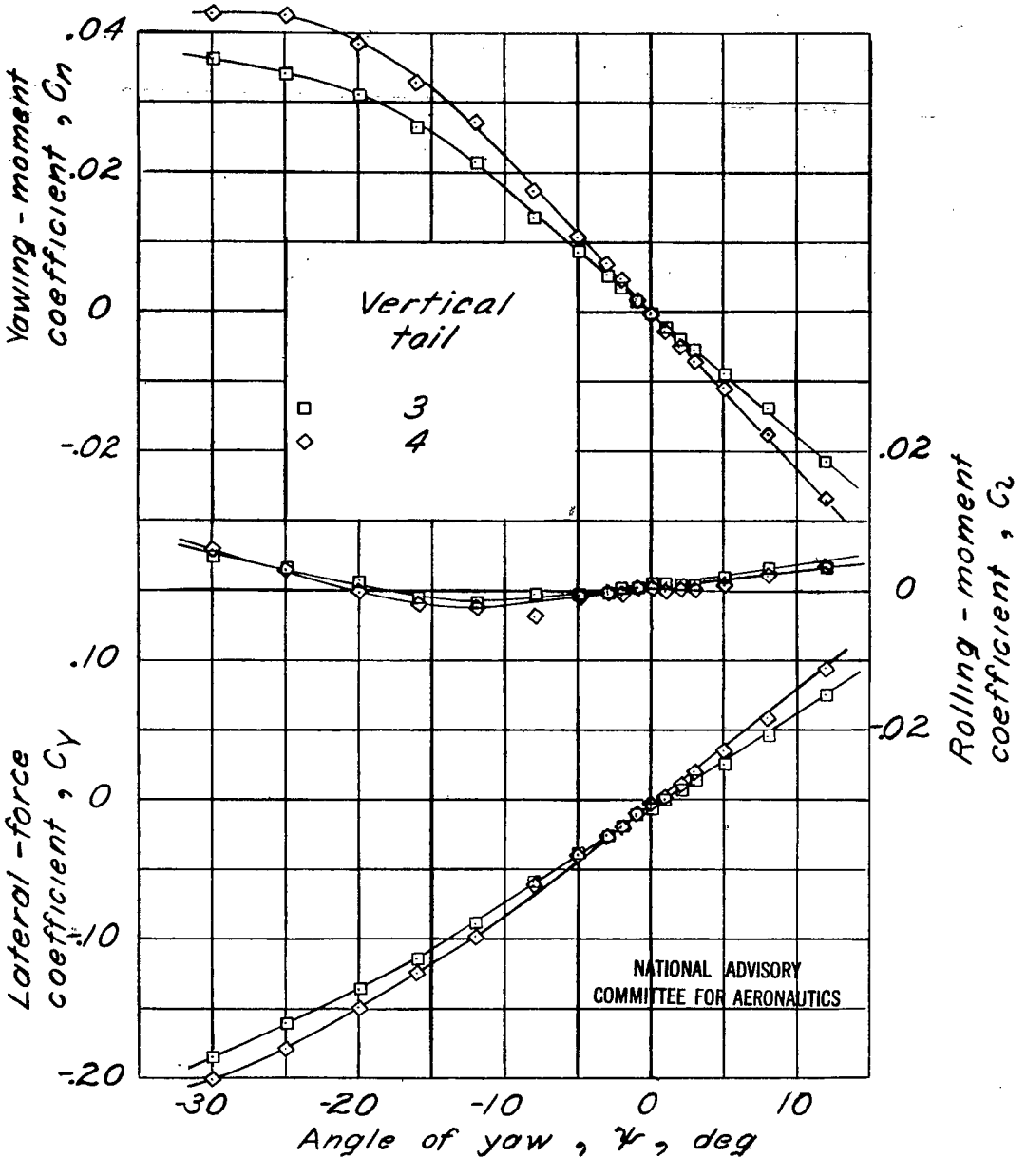

(a) Γ, 0°.

Figure 17. - Effect of changing vertical-tail area on variation of yawing-moment, rolling-moment, and lateral-force coefficients with angle of yaw. Medium-length fuselage with horizontal tail; α, 10.2°; q, 65 lb/sq ft.

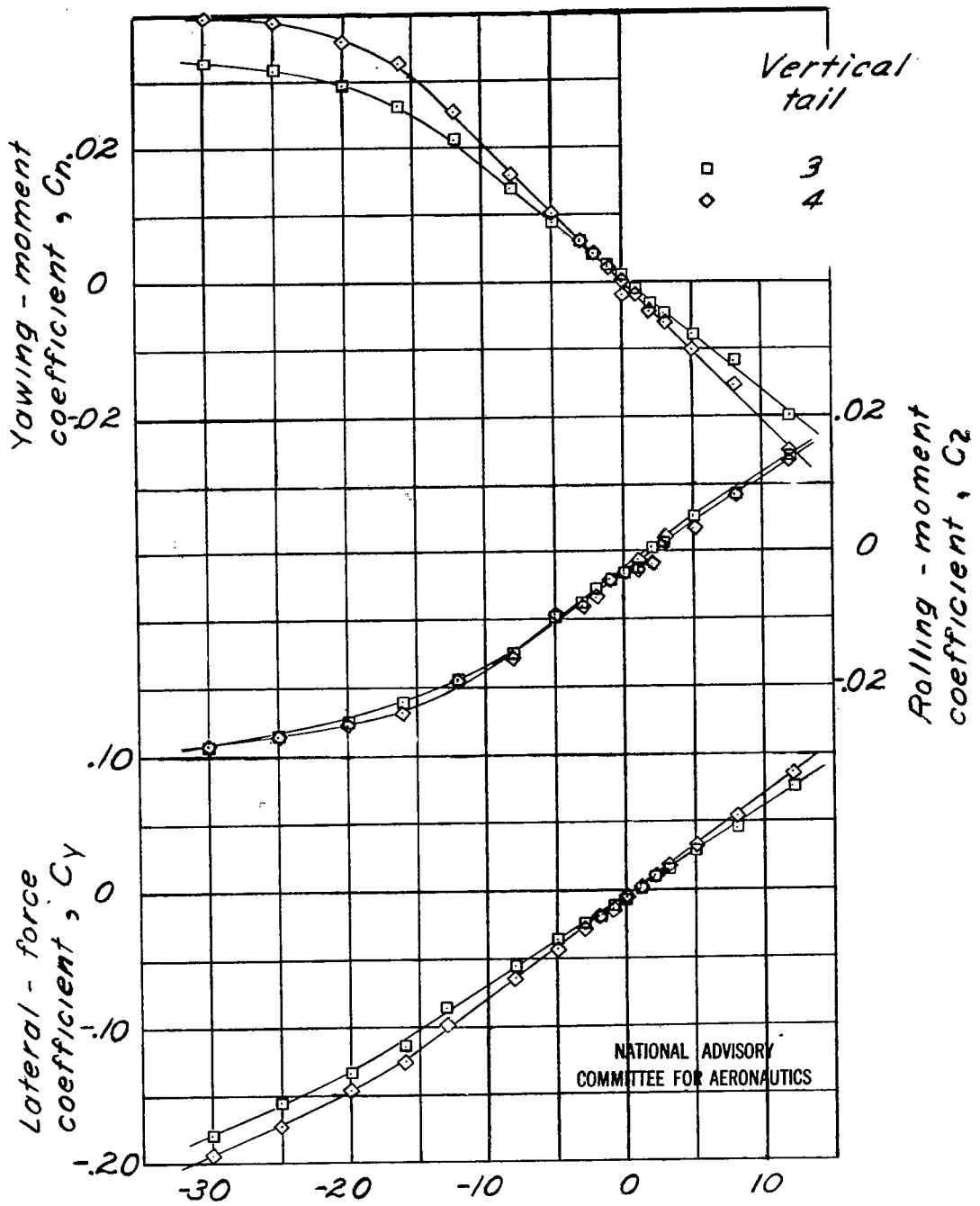

(b) Γ, 5°.

Figure 17 .- Concluded .

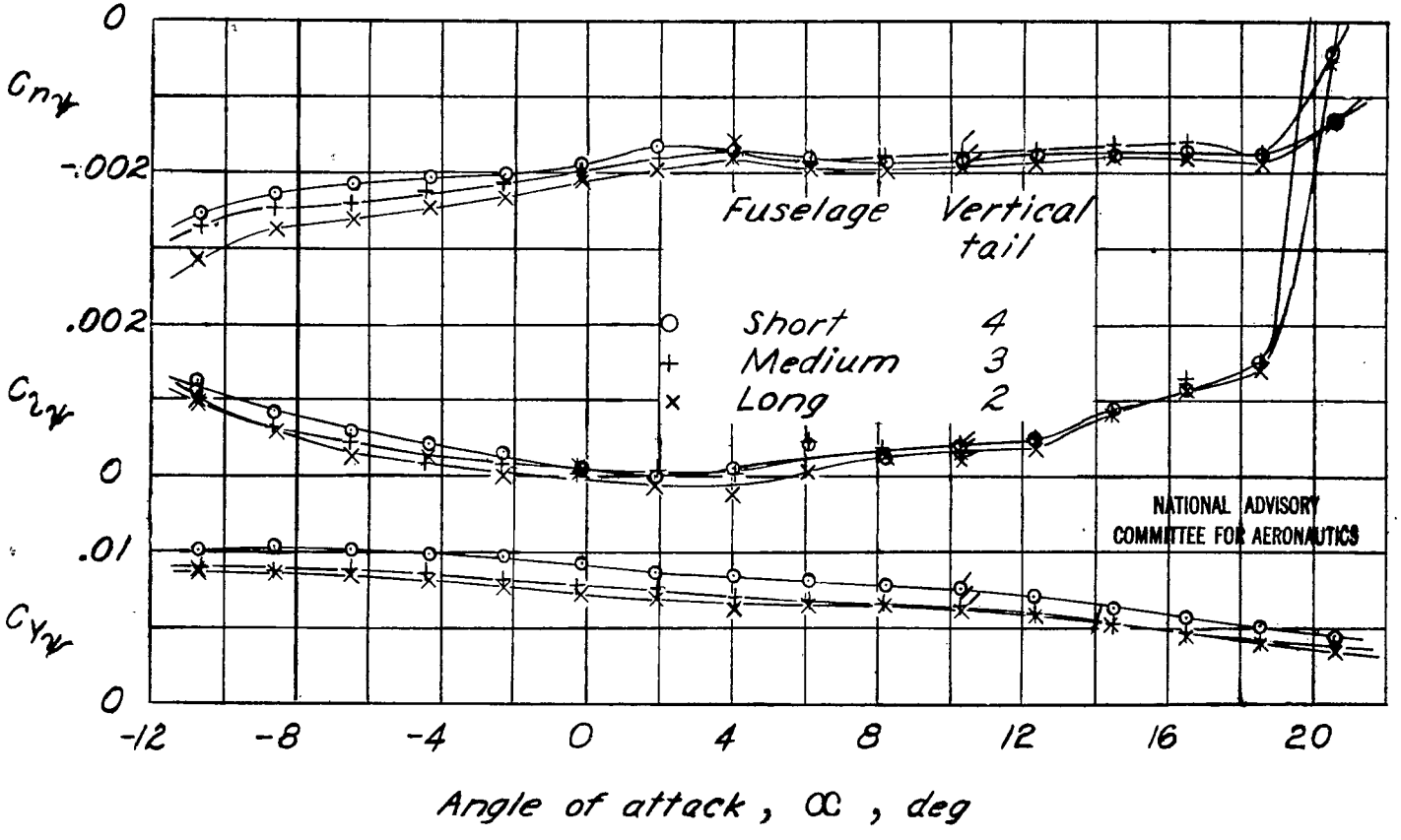

(a) Γ, 0°.

Figure 18.- Effect of several combinations having constant tail volume on variation of lateral-stability slopes C_{n_ψ}, C_{l_ψ}, and C_{Y_ψ} with angle of attack. Tail volume, 0.0407; horizontal tail on; q, 65 lb/sq ft.

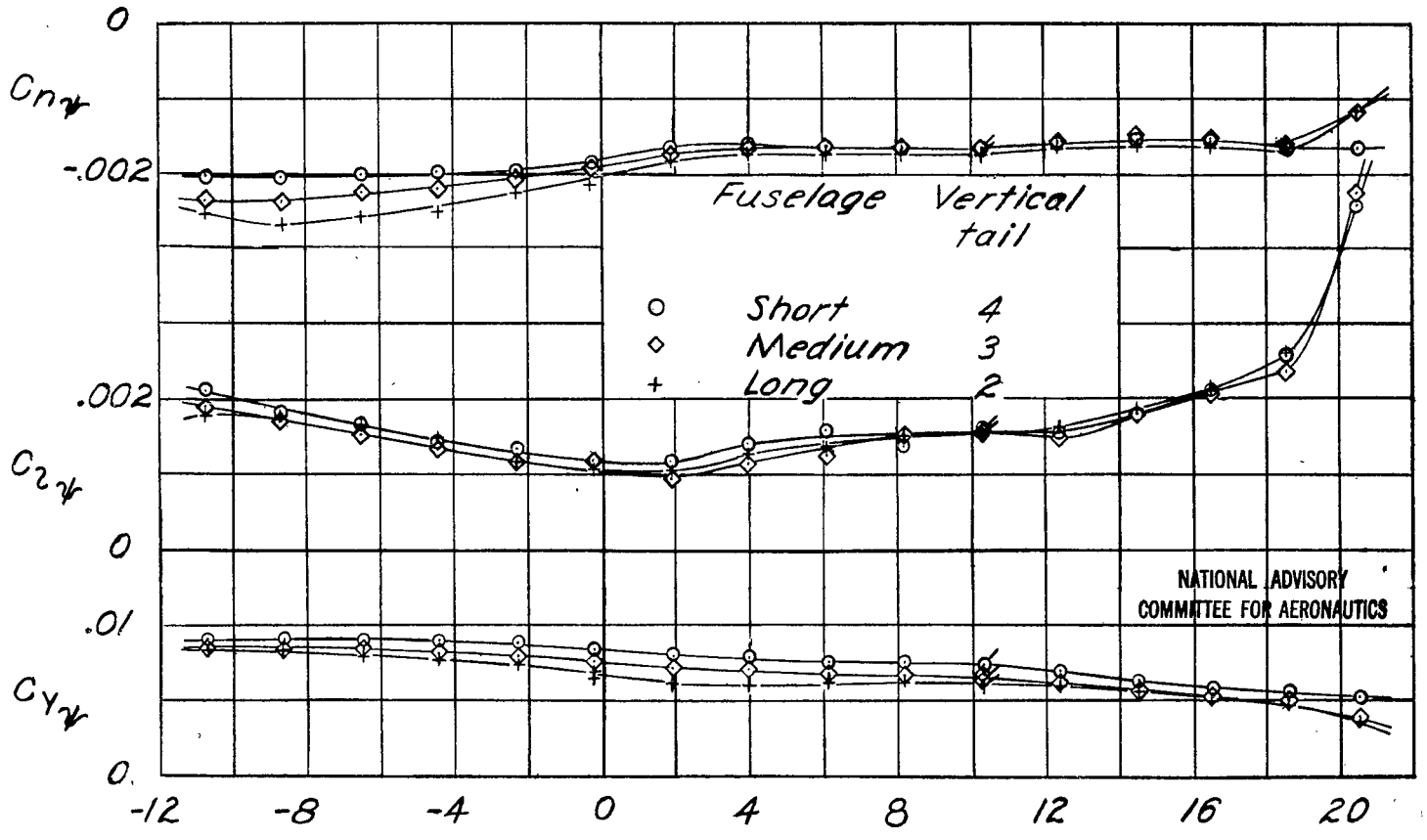

(b) Γ, 5°.

Figure 18.- Concluded.

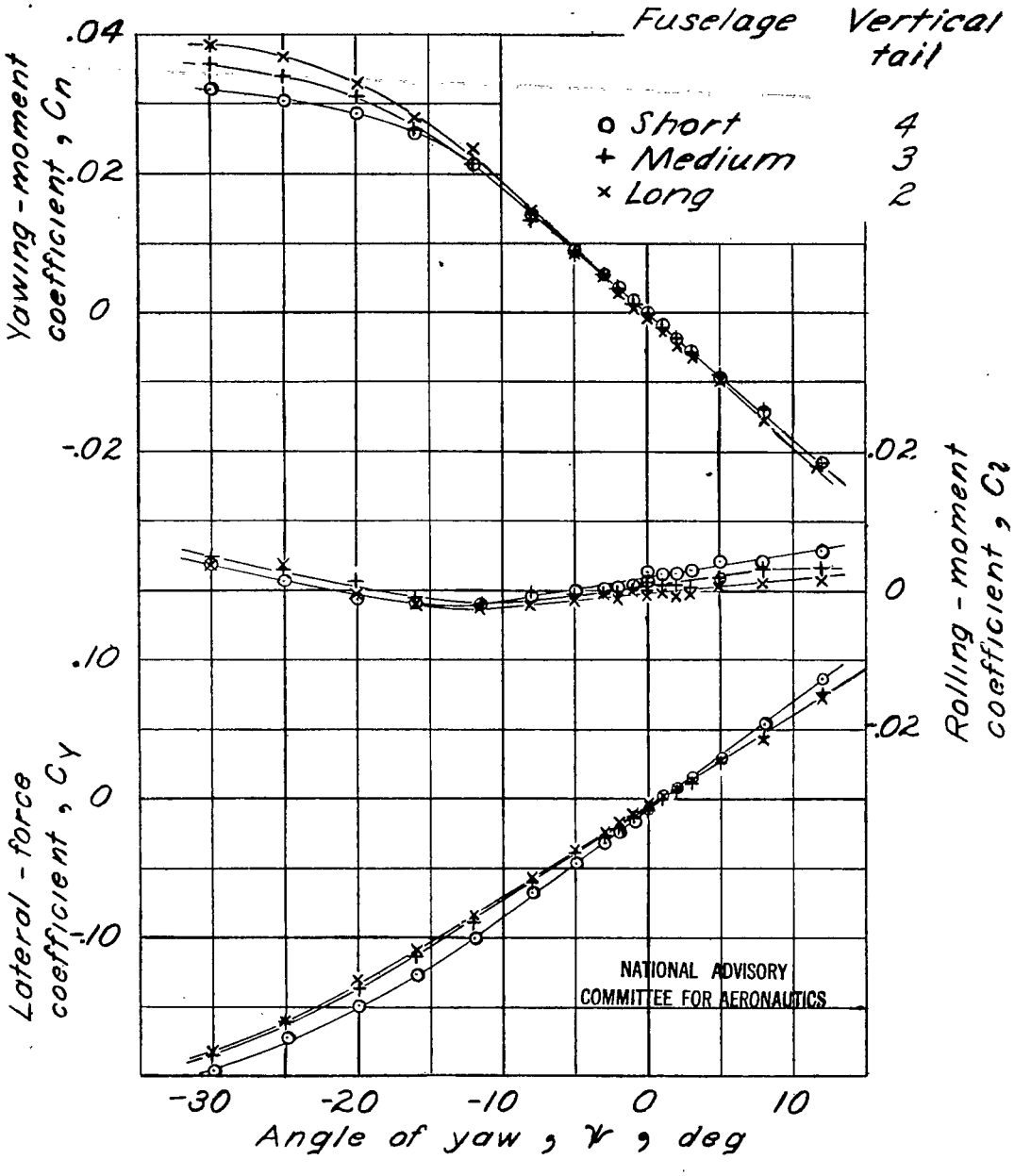

(a) Γ, 0°.

Figure 19.- Effect of several combinations having constant tail volume on variation of yawing-moment, rolling-moment, and lateral-force coefficients with angle of yaw. Tail volume, 0.0407; horizontal tail on; α, 10.2°; q, 65 lb/sq ft.

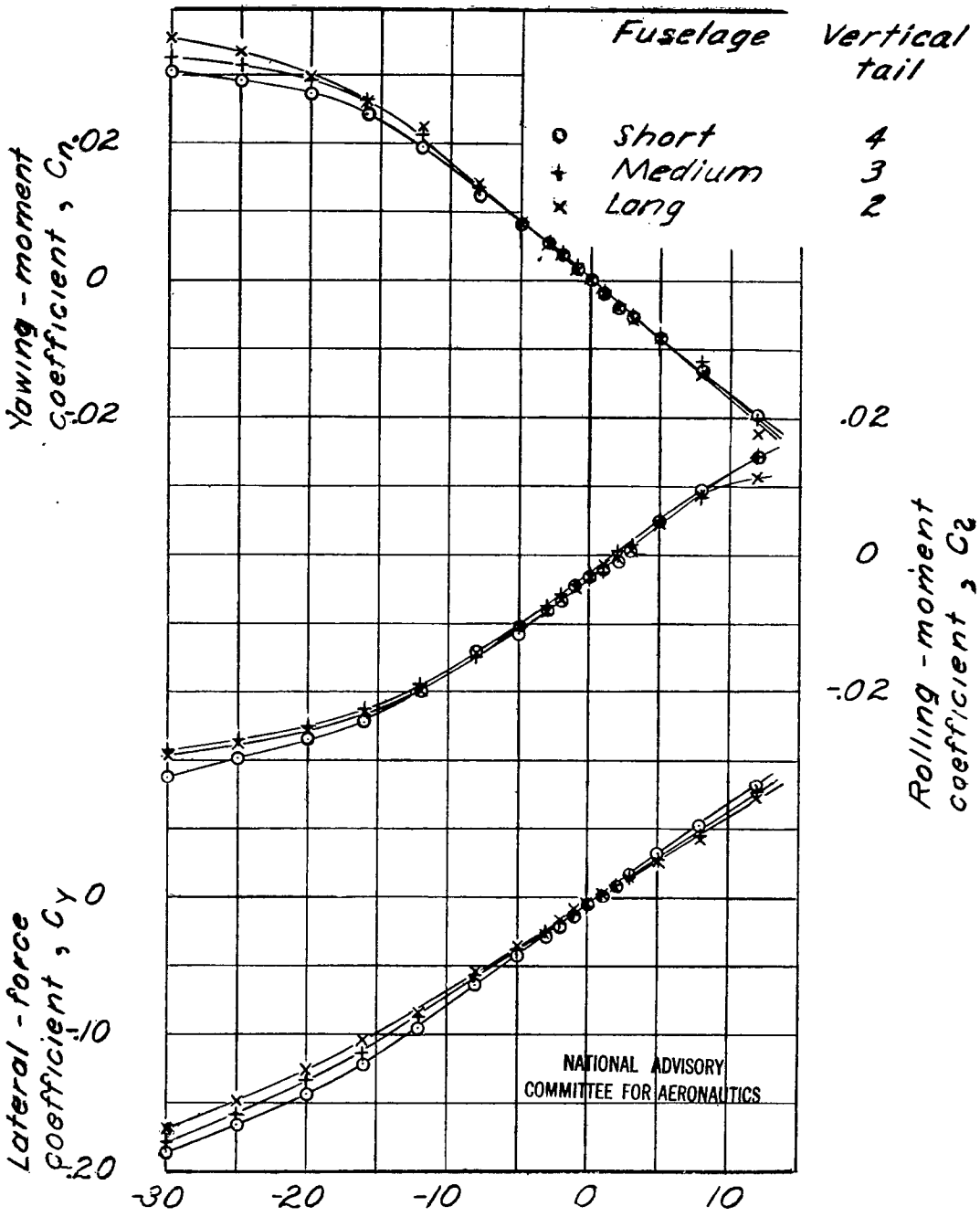

(b) Γ, 5°.

Figure 19.- Concluded.

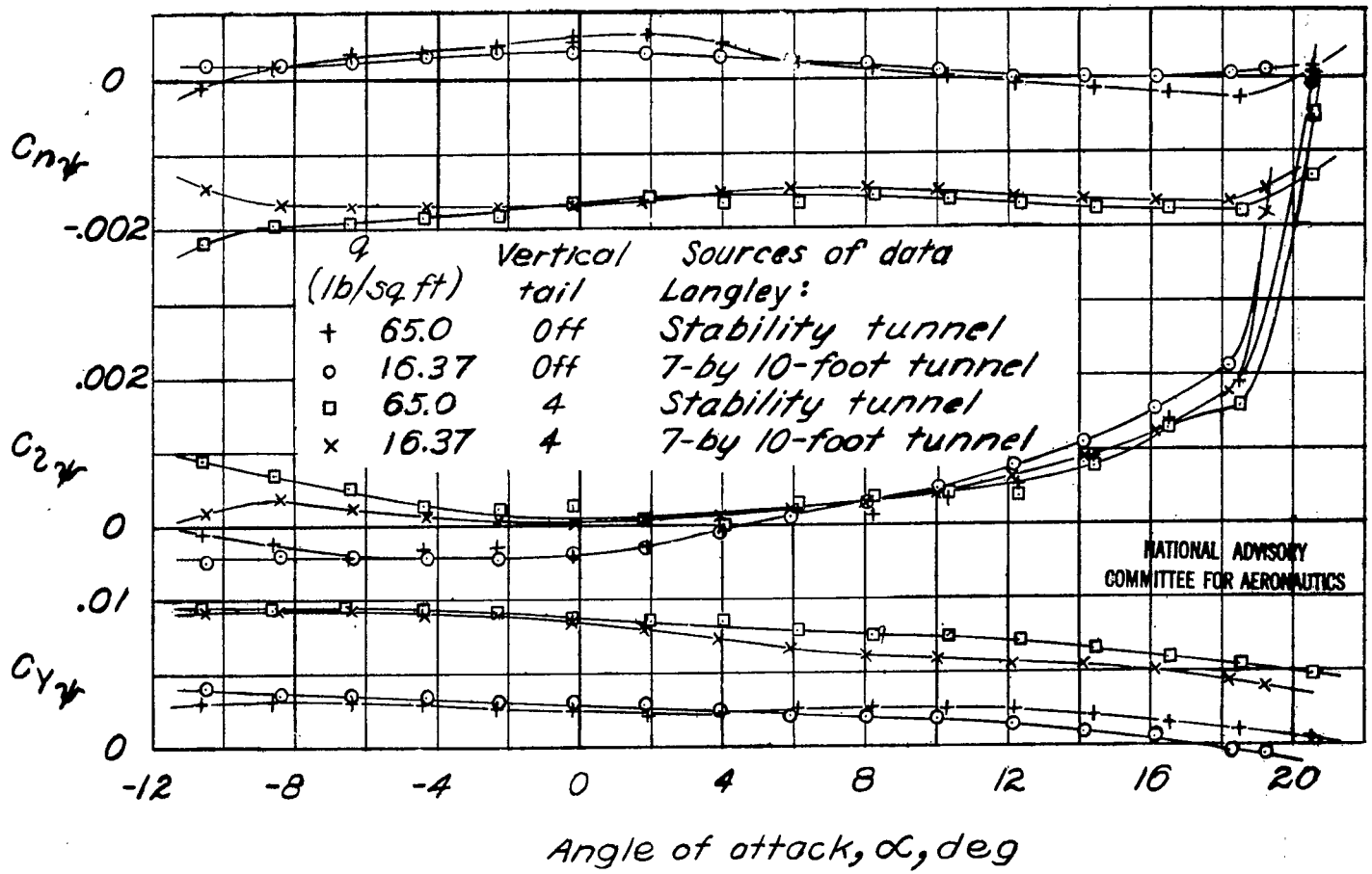

Figure 20.- Comparison of data from Langley stability and Langley 7-by 10-foot tunnels for variation of lateral-stability slopes C_{n_ψ}, C_{l_ψ}, and C_{Y_ψ} with angle of attack. Short fuselage in combination with rectangular wing; horizontal tail off; Γ, 0°.